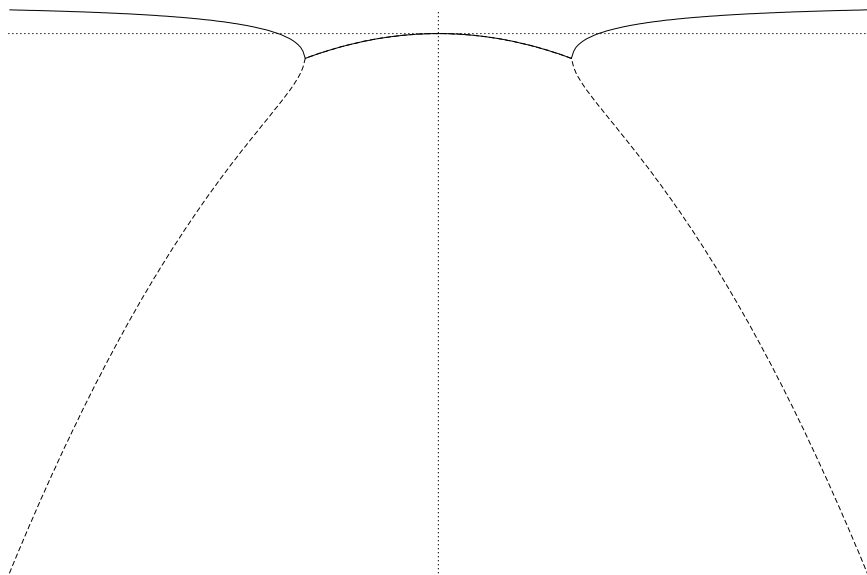
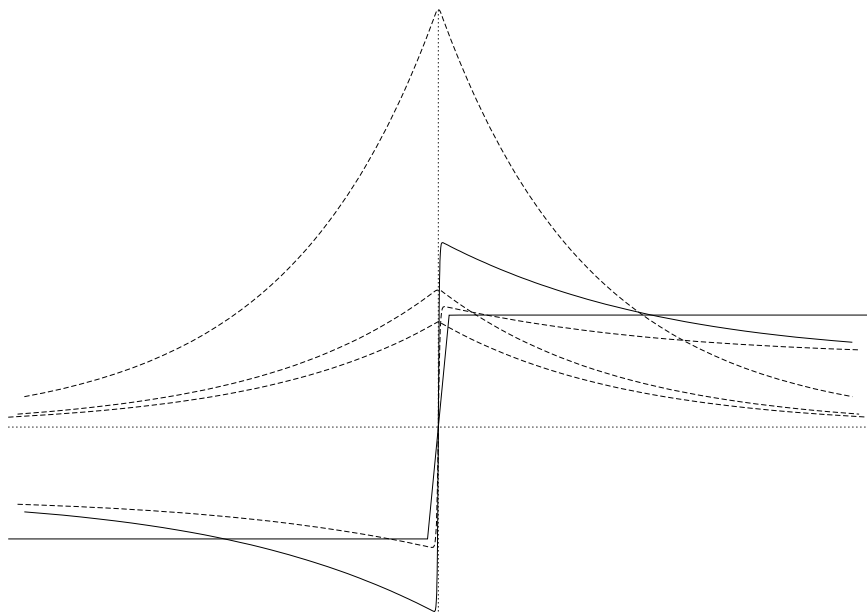




com



k



DESTABILIZATION OF FRONTS IN A CLASS OF BI-STABLE SYSTEMS

ARJEN DOELMAN*[†], DAVID IRON*[‡] AND YASUMASA NISHIURA[‡]

Abstract. In this article, we consider a class of bi-stable reaction-diffusion equations in two components on the real line. We assume that the system is singularly perturbed, i.e. that the ratio of the diffusion coefficients is (asymptotically) small. This class admits front solutions that are asymptotically close to the (stable) front solution of the ‘trivial’ scalar bi-stable limit system $u_t = u_{xx} + u(1 - u^2)$. However, in the system these fronts can become unstable by varying parameters. This destabilization is either caused by the essential spectrum associated to the linearized stability problem, or by an eigenvalue that exists near the essential spectrum. We use the Evans function to study the various bifurcation mechanisms and establish an explicit connection between the character of the destabilization and the possible appearance of saddle-node bifurcations of heteroclinic orbits in the existence problem.

Key words. pattern formation, bi-stable systems, geometric singular perturbation theory, stability analysis, Evans functions

AMS subject classifications. 35B25, 35B32, 35B35, 35K57, 35P20, 34A26, 34C37

1. Introduction. The class of bi-stable reaction-diffusion equations we consider in this paper is given by

$$\begin{cases} U_t &= \varepsilon^2 U_{xx} + (1 + V - U^2)U \\ \tau V_t &= V_{xx} + F(U^2, V; \varepsilon), \end{cases} \quad (1.1)$$

where $F(U^2, V; \varepsilon)$ is a smooth function of U^2 , V and ε such that $F(1, 0; \varepsilon) \equiv 0$ and $\lim_{\varepsilon \rightarrow 0} F(U^2, V; \varepsilon)$ exists; $\tau > 0$ is a parameter. Thus, the system is such that the background state $(U, V) \equiv (\pm 1, 0)$ is always a solution. We furthermore assume that the ratio of the two diffusion coefficients, ε^2 , is asymptotically small, thus the problem has a singularly perturbed nature. We consider the system on the (unbounded) line, i.e. $(U, V) = (U(x, t), V(x, t))$ with $(x, t) \in \mathbb{R} \times \mathbb{R}^+$. Note that (1.1) is (by construction) symmetric under

$$U \rightarrow -U. \quad (1.2)$$

To motivate the structure of (1.1) we introduce the fast variable

$$\xi = \frac{x}{\varepsilon}, \quad (1.3)$$

so that (1.1) can be written in its equivalent ‘fast’ form

$$\begin{cases} U_t &= U_{\xi\xi} + (1 + V - U^2)U \\ \varepsilon^2 \tau V_t &= V_{\xi\xi} + \varepsilon^2 F(U^2, V; \varepsilon). \end{cases} \quad (1.4)$$

Since $U(x, t)$ and $V(x, t)$ are a priori supposed to be bounded on the entire domain $\mathbb{R} \times \mathbb{R}^+$, we find in the natural (fast reduced) limit, i.e. $\varepsilon \rightarrow 0$ in (1.4), that $V \equiv V_0$ and that U is a solution of the well-studied, scalar (standard) bi-stable or Nagumo equation,

$$U_t = U_{\xi\xi} + (1 + V_0 - U^2)U. \quad (1.5)$$

In this paper we interpret the original system, (1.1) or (1.4), as a scalar bi-stable Nagumo equation (1.5) in which the coefficient of the linear term is allowed to evolve by reaction and diffusion on a

*Korteweg-deVries Instituut, Universiteit van Amsterdam, Plantage Muidergracht 24, 1018 TV Amsterdam, the Netherlands

[†]Centrum voor Wiskunde en Informatica, P.O. Box 94079, 1090 GB Amsterdam, the Netherlands

[‡]Laboratory of Nonlinear Studies and Computation, Research Institute for Electronic Science, Hokkaido University, Kita-ku, Sapporo, 060, Japan

long, or slow, spatial scale. Note that the (slow) dynamics of the V -component are allowed to be completely general, except that it is assumed that the full system conserves the symmetry (1.2) and the background states $U \equiv \pm 1$, at $V \equiv 0$, of the scalar limit (see also Remark 1.1). A priori, one expects that the V -component of front-like solutions will remain small ($\mathcal{O}(\varepsilon)$) due to the ‘boundary conditions’ $V = 0$ at $\pm\infty$, so that the effect of the slowly varying $V(x, t)$ -component cannot have a significant influence on the (well-understood) dynamics of the scalar Nagumo equation. An important motivation of the research in this paper is to find out whether or not this intuition is correct.

We will focus completely on the existence and stability issues associated to the persistence of the asymptotically stable stationary front solutions of the bi-stable equation (1.5) with $V_0 = 0$. In fact, this paper can also be seen as a first step towards analyzing the dynamics (and possibly defects) of striped patterns in a class of relatively simple bi-stable reaction-diffusion equations, i.e. (1.1) for $(U, V) = (U(x, y, t), V(x, y, t))$ with $(x, y) \in \mathbb{R}^2$. The methods and techniques developed in this paper are supposed to carry over to the analysis of the existence and stability of spatially periodic solutions of (1.1) and their two-dimensional counterparts (the planar fronts and the stripe patterns). See also section 5.

The problem of the persistence of the stable front solution of the scalar bi-stable equation (1.5) is quite subtle, as can be expected in the light of recent results on the stability of pulses in singularly perturbed reaction-diffusion equations of the Gray-Scott and Gierer-Meinhardt type [4, 5]. Such systems can also be written in the form (1.4), however, the scalar limit systems are mono-stable, i.e. in essence of the form $U_t = U_{\xi\xi} - U + U^2$. The pulses correspond in this (fast reduced) limit to the stationary homoclinic solution of $u_{\xi\xi} - u + u^2 = 0$. Thus, one would expect that the pulses of the full system cannot be stable, since the stability problem associated to the homoclinic solution has an $\mathcal{O}(1)$ unstable eigenvalue. Nevertheless, stable pulses of this type do exist in the Gray-Scott and the Gierer-Meinhardt equation [4, 5]. On the other hand, the stability of the pulses in these mono-stable equations is strongly related to the freedom one has in these systems to scale the magnitude of the pulses, i.e. the amplitude of the stable pulses is asymptotically large in ε in these mono-stable systems. Such scalings are not possible for the fronts in the bi-stable case, since the background states $(\pm 1, 0)$ are fixed (and $\mathcal{O}(1)$).

In the analysis of the front solutions, we will find that it is natural to decompose $F(U^2, V; \varepsilon)$ into a component that has a factor of $(1 + V - U^2)$ and a rest term $G(V; \varepsilon)$ that does not depend on U^2 . Hence, we write (1.1) as,

$$\begin{cases} U_t &= \varepsilon^2 U_{xx} + (1 + V - U^2)U \\ \tau V_t &= V_{xx} + (1 + V - U^2)H(U^2, V; \varepsilon) + G(V; \varepsilon), \end{cases} \quad (1.6)$$

with $G(0, \varepsilon) \equiv 0$. Note that this decomposition induces no restriction on $F(U^2, V; \varepsilon)$ since we have assumed that F is smooth. In fact

$$G(V) = F(1 + V, V) \quad \text{and} \quad (1 + V - U^2)H(U^2, V) = F(U^2, V) - F(1 + V, V).$$

We will find that the quantities $\frac{\partial G}{\partial V}(0; \varepsilon)$ and $H(1, 0; \varepsilon)$ have a crucial impact on the structure and the dynamics of the front-like solutions. Therefore, we define

$$G_1(\varepsilon) = \frac{\partial G}{\partial V}(0; \varepsilon) \quad \text{and} \quad H_0 = H(1, 0; \varepsilon); \quad (1.7)$$

G_1 is the main bifurcation parameter used in this paper. Throughout this paper we assume that $H(U^2, V)$ is non-degenerate, i.e. that $H(1 + V, V)$ is not identically 0, and that $\tau = \mathcal{O}(1)$ (see Remark 4.13).

In section 2 we will show that as long as $G_1 < 0$ and $\mathcal{O}(1)$, the front solutions of (1.5) with $V_0 = 0$ persist in a regular fashion, in the sense that the system (1.1) has front solution with U -components that are asymptotically and uniformly close to a front in (1.5) with $V_0 = 0$, and with V -components that are asymptotically and uniformly small (Theorem 2.1). However, if G_1

becomes $O(\varepsilon^2)$ these fronts become truly singular, in the sense that V becomes $\mathcal{O}(1)$, while the U -component is close to a front of (1.5) with $V_0 \neq 0$, on the fast spatial scale (and it converges to $U = \pm 1$ on the slow spatial scale). Moreover, the front solutions are no longer uniquely determined, there can be several types of heteroclinic front solutions if $G_1 = \mathcal{O}(\varepsilon^2)$ that may or may not merge in saddle-node bifurcations of heteroclinic orbits when G_1 is varied (Theorems 2.3 and 2.5). It should be noted here that we for simplicity consider $G(V) = -\varepsilon^2\gamma V$ in (1.1) in the singular limit $G_1 = \mathcal{O}(\varepsilon^2)$ although this paper – see Remark 2.4. We refer to Figure 1 for a numerical representation of a regular front (Figure 1a) and a singular front (Figure 1b). The magnitude of

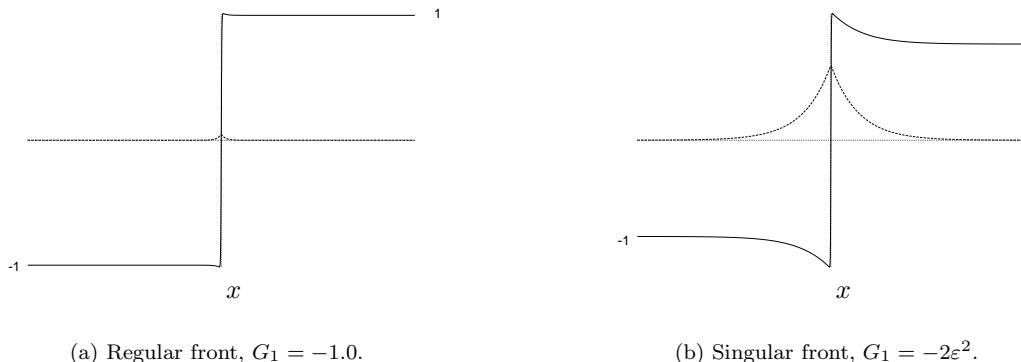


FIG. 1.1. Two asymptotically stable front solutions of (1.1)/(1.6) plotted on the slow spatial scale x (by a numerical simulation). Here $H(U^2, V) = H_0U^2$, $G(V) = G_1V$, $\varepsilon = 0.1$ and $H_0 = 1$. The solid curves represent the U -coordinates, the dotted curves the V -coordinates.

G_1 is also extremely relevant in the stability analysis. It can be shown that the (regular) front solutions are asymptotically stable as long as $G_1 < 0$ and $\mathcal{O}(1)$ and $H_0 + G_1 - 2\tau < 0$ and $\mathcal{O}(1)$ – Theorem 4.3. It seems, at leading order, that the destabilization of the front is caused by the essential spectrum, σ_{ess} , associated to the stability of the front (σ_{ess} reaches the imaginary axis exactly at $G_1 = 0$ or at $H_0 + G_1 - 2\tau = 0$ – Lemma 3.2). However, the analysis also shows that there can be eigenvalues near the ‘tips’ of σ_{ess} , and that it is possible that the destabilization is caused by such an eigenvalue, i.e. by an element of the discrete spectrum and not by σ_{ess} . These ‘new’ eigenvalues do not have counterparts in the (scalar) fast reduced limit problem, they have a singular slow-fast nature and may appear through edge bifurcations from the essential spectrum.

In section 4 we study in detail the nature of the destabilization as $G_1 < 0$ increases towards 0. In this section it becomes clear that there is an intimate relation between the geometrical character of the singularly perturbed existence problem and the character of the destabilization of the front. This is a natural and frequently encountered relation – see for instance [13] and the references there. We establish that a front solution destabilizes at a critical value of $G_1 = -\varepsilon^2\gamma_{\text{double}} < 0$ by an eigenvalue if and only if it merges with another front solution in a saddle-node bifurcation of heteroclinic orbits. Moreover, we are able to determine the explicit value of this bifurcation value $\gamma_{\text{double}} > 0$. If the front does not ‘encounter’ such a saddle-node as G_1 increase to 0, the front will be destabilized by σ_{ess} at $G_1 = 0$ – see Theorems 4.6 and 4.10.

Another way to motivate the analysis of this paper is as follows. In this paper we show that the technique of decomposing the Evans function associated to the stability of a ‘localized structure’ (a (traveling) pulse or front) into the product of an analytic ‘fast’ and a meromorphic ‘slow’ transmission function ([4, 5]) can be extended to a class of bi-stable equations. We show that the slow transmission function ($t_2(\lambda, \varepsilon)$) is a natural tool for analyzing the existence or appearance of eigenvalues near or from the essential spectrum, and that such eigenvalues play a crucial role in the stability of the front. Note that in this sense, the theme of this paper is similar to that of [14], where Evans function techniques are developed to study eigenvalues near σ_{ess} in a class of nearly

integrable systems.

The paper is organized as follows. The existence problem is studied in section 2. In section 3 the basic properties of the linearized stability problem are studied and (the decomposition of) the Evans function is introduced. Section 4 is the main section of the paper, in it we develop an approach by which the (possible) location and existence of ‘slow-fast eigenvalues’ near the essential spectrum can be studied. This section is split into three parts: a subsection on the regular problem, a subsection in which we study an explicit example ($G(V) = -\varepsilon^2\gamma$, $H(U^2, V) = H_0U^2$) in full detail, and a subsection in which we study the ‘fate’ of the regular front as G_1 approaches 0 in the general case. In section 5 we present simulations which clearly exhibit the impact of the distinction between a destabilization by the discrete or by the essential spectrum. Moreover, we discuss some related issues and topics of future research.

REMARK 1.1. Large parts of the theory developed in this paper can be generalized to systems of the type (1.1)/(1.4) in which the fast reduced limit system is of the type $U_t = U_{\xi\xi} + B(U^2; V_0)U$ for some function B , i.e. to bi-stable systems of a more general nature. We focused on the standard case, i.e. $B = 1 + V_0 - U^2$, since the analysis is more transparent. If one drops the condition on the symmetry (1.2), the fronts will in general travel with a certain (nonzero) speed. Although the symmetry is used throughout this paper, there is no reason to expect that such asymmetric systems cannot be studied along the lines of the methods presented here.

2. The existence problem. We analyze the existence of stationary one-dimensional patterns through geometric singular perturbation theory [9, 11] using the methods developed in [6, 5]. Therefore, we write the ODE associated to (1.6) as a dynamical system in \mathbb{R}^4 ,

$$\begin{cases} \dot{u} &= p \\ \dot{p} &= -(1 + v - u^2)u \\ \dot{v} &= \varepsilon q \\ \dot{q} &= \varepsilon [-(1 + v - u^2)H(u^2, v; \varepsilon) - G(v; \varepsilon)], \end{cases} \quad (2.1)$$

where $\dot{\cdot}$ denotes the derivative with respect to the spatial variable ξ (1.3) (i.e. ξ ‘plays the role of time’). Note that this system inherits two symmetries of (1.6)

$$\xi \rightarrow -\xi, p \rightarrow -p, q \rightarrow -q \text{ and } u \rightarrow -u, v \rightarrow v. \quad (2.2)$$

We consider the ‘super-slow’ case in which $G_1(\varepsilon) = \mathcal{O}(\varepsilon^2)$ separately in sections 2.2 and 2.3. Note that in the fast reduced limit, i.e. $\varepsilon \rightarrow 0$ in (2.1), the monotonically increasing heteroclinic front solution is given by (u_0, p_0, v_0, q_0) , where

$$(u_0(\xi; v_0), p_0(\xi; v_0)) = \left(\sqrt{1 + v_0} \tanh \left(\sqrt{\frac{1 + v_0}{2}} \xi \right), \frac{1 + v_0}{\sqrt{2}} \operatorname{sech}^2 \left(\sqrt{\frac{1 + v_0}{2}} \xi \right) \right), \quad (2.3)$$

and v_0 and q_0 are constants.

2.1. The regular case. The main result of this section is,

THEOREM 2.1. *Let $G_1(\varepsilon)$ (1.7) be $\mathcal{O}(1)$ and negative. Then, for $\varepsilon > 0$ small enough, system (2.1) has a symmetric pair of heteroclinic orbits: $\Gamma_h^+(\xi; \varepsilon) = (u_h(\xi; \varepsilon), p_h(\xi; \varepsilon), v_h(\xi; \varepsilon), q_h(\xi; \varepsilon))$ and $\Gamma_h^-(\xi; \varepsilon) = (-u_h(\xi; \varepsilon), -p_h(\xi; \varepsilon), v_h(\xi; \varepsilon), q_h(\xi; \varepsilon))$, with $\lim_{\xi \rightarrow \pm\infty} \Gamma_h^+(\xi; \varepsilon) = (\pm 1, 0, 0, 0)$ and $\lim_{\xi \rightarrow \pm\infty} \Gamma_h^-(\xi; \varepsilon) = (\mp 1, 0, 0, 0)$; $u_h(\xi; \varepsilon)$ and $q_h(\xi; \varepsilon)$ are odd and monotonic as functions of ξ , $v_h(\xi; \varepsilon)$ and $p_h(\xi; \varepsilon)$ even. Moreover, $|u_h(\xi; \varepsilon) - u_0(\xi; 0)| = \mathcal{O}(\varepsilon)$ (2.3) uniformly on \mathbb{R} , $|v_h(\xi; \varepsilon)|, |q_h(\xi; \varepsilon)| = \mathcal{O}(\varepsilon)$ uniformly on \mathbb{R} , and $v_h(0; \varepsilon)$ is the extremal value of $v_h(\xi; \varepsilon)$, with*

$$v_h(0; \varepsilon) = \frac{\varepsilon}{2\sqrt{-G_1(0)}} \int_{-\infty}^{\infty} (1 - u_0^2(\xi; 0)) H(u_0^2(\xi; 0), 0) d\xi + \mathcal{O}(\varepsilon^2). \quad (2.4)$$

The orbits $\Gamma^\pm(\xi; \varepsilon)$ correspond to the (stationary) front patterns $(\pm U_h(\xi; \varepsilon), V_h(\xi; \varepsilon))$ of (1.6) with $U_h(\xi; \varepsilon) = u_h(\xi; \varepsilon)$ odd as function of ξ , $V_h(\xi; \varepsilon) = v_h(\xi; \varepsilon) = \mathcal{O}(\varepsilon)$ even, $\lim_{\xi \rightarrow \pm\infty} U_h(\xi; \varepsilon) = \pm 1$, and $\lim_{\xi \rightarrow \pm\infty} V_h(\xi; \varepsilon) = 0$.

Proof. As the system is singularly perturbed, we also consider (2.1) with the slow scaling $x = \varepsilon\xi$, (2.1) is given by,

$$\begin{cases} \varepsilon u' &= p \\ \varepsilon p' &= -(1 + v - u^2)u \\ v' &= q \\ q' &= [-(1 + v - u^2)H(u^2, v; \varepsilon) - G(v; \varepsilon)], \end{cases} \quad (2.5)$$

where ' refers to differentiation with respect x . System (2.5) is referred to as the slow system. We begin by finding the locally invariant manifolds of (2.5) in the limit $\varepsilon \rightarrow 0$. In this limit, the first two equations of (2.5) will reduce to,

$$p = 0, \quad -(1 + v - u^2)u = 0. \quad (2.6)$$

The manifold given by $(u, p, v, q) = (0, 0, v, q)$ is not normally hyperbolic and will not be considered. However, the manifolds, denoted \mathcal{M}_0^\pm , determined by $(u, p, v, q) = (\pm\sqrt{1+v}, 0, v, q)$ are normally hyperbolic and thus by [9, 11], (2.5) possesses locally invariant manifolds $\mathcal{M}_\varepsilon^\pm$, which are $\mathcal{O}(\varepsilon)$ close to \mathcal{M}_0^\pm . We now determine the leading order correction to these manifolds. Let the manifold $\mathcal{M}_\varepsilon^\pm$, be given by,

$$\mathcal{M}_\varepsilon^\pm = \{u = \pm\sqrt{1+v} + \varepsilon U^\pm(v, q; \varepsilon), p = \varepsilon P^\pm(v, q; \varepsilon), v, q\}. \quad (2.7)$$

To obtain successive approximations of $\mathcal{M}_\varepsilon^\pm$, we can expand $U^\pm = u_1^\pm + \varepsilon u_2^\pm + \dots$, and $P^\pm = p_1^\pm + \varepsilon p_2^\pm + \dots$. Using the first two lines of (2.5) we find,

$$p_1^\pm = \frac{q}{2\sqrt{1+v}}, \quad p_2^\pm = \frac{\partial u_1^\pm}{\partial v} q - \frac{\partial u_1^\pm}{\partial q} G(v; \varepsilon), \quad u_1^\pm = 0, \quad u_2^\pm = \mp \frac{q^2}{4(1+v)^{5/2}} \mp \frac{G(v; \varepsilon)}{(1+v)^{3/2}}. \quad (2.8)$$

Hence, the (slow) flow on the slow manifold is given by,

$$v'' = -G(v; \varepsilon) + \mathcal{O}(\varepsilon^2). \quad (2.9)$$

To leading order, this flow is integrable. The point $(v, q) = (0, 0)$, that corresponds to $(\pm 1, 0, 0, 0)$, is a critical point on $\mathcal{M}_\varepsilon^\pm$. Since $G_1 < 0$, $(0, 0)$ is a saddle on $\mathcal{M}_\varepsilon^\pm$ with stable direction $(1, \sqrt{-G_1})$ and unstable direction $(-1, \sqrt{-G_1})$.

A heteroclinic orbit Γ_h^\pm from $(\mp 1, 0, 0, 0)$ to $(\pm 1, 0, 0, 0)$ is both an element of $W^u(\mathcal{M}_\varepsilon^\mp)$ and of $W^s(\mathcal{M}_\varepsilon^\pm)$. Here we will only consider Γ_h^+ . The existence of Γ_h^- follows from the symmetry (2.2). The orbit Γ_h^+ remains exponentially close to $W^u(-1, 0, 0, 0)|_{\mathcal{M}_\varepsilon^-}$ before it 'takes off' and makes a 'jump' through the fast field. After that, it 'touches down' on $\mathcal{M}_\varepsilon^+$ and remains exponentially close to it (and to $W^u(1, 0, 0, 0)|_{\mathcal{M}_\varepsilon^+}$ - see Figure 2.1. The change in q by the passage through the fast field is $\mathcal{O}(\varepsilon)$ (2.1), therefore Γ_h^+ must take off from $\mathcal{M}_\varepsilon^-$ and touch down on $\mathcal{M}_\varepsilon^+$ with a q -coordinate that is $\mathcal{O}(\varepsilon)$. Since Γ_h^+ is asymptotic to the saddle points $(0, 0) \in \mathcal{M}_\varepsilon^\pm$, it follows that the v -coordinate of Γ_h^+ must also be $\mathcal{O}(\varepsilon)$. Note that we have used here implicitly that $G_1 = \mathcal{O}(1)$.

We will determine whether such a trajectory, as Γ_h^+ , is possible using a Melnikov method. Both $W^u(\mathcal{M}_\varepsilon^-)$ and $W^s(\mathcal{M}_\varepsilon^+)$ are $\mathcal{O}(\varepsilon)$ close to the family of heteroclinic orbits in the fast reduced limit of (2.1) given in (2.3). The leading order distance between $W^u(\mathcal{M}_\varepsilon^-)$ and $W^s(\mathcal{M}_\varepsilon^+)$ can be determined by a Melnikov function for slowly varying systems [18]. Both $W^u(\mathcal{M}_\varepsilon^-)$ and $W^s(\mathcal{M}_\varepsilon^+)$ intersect the hyperplane $\{u = 0\}$ transversally. Note that $W^{s,u}(\mathcal{M}_\varepsilon^\pm) \cap \{u = 0\}$ is 2-dimensional, thus, since $\{u = 0\}$ is 3-dimensional, one expects a 1-dimensional intersection $W^u(\mathcal{M}_\varepsilon^-) \cap W^s(\mathcal{M}_\varepsilon^+) \cap \{u = 0\}$. The separation between $W^u(\mathcal{M}_\varepsilon^-)$ and $W^s(\mathcal{M}_\varepsilon^+)$ is, at leading order, measured by the integral,

$$\Delta = \int_{-\infty}^{\infty} \begin{pmatrix} p(\xi) \\ u(\xi) + u^3(\xi) - u(\xi)v_0 \end{pmatrix} \wedge \begin{pmatrix} 0 \\ -u(\xi)\frac{\partial q}{\partial \delta}(\xi) \end{pmatrix} d\xi. \quad (2.10)$$

Here the wedge product refers to the scalar cross product and $\frac{\partial q}{\partial \delta}$ solves the differential equation, $\frac{d}{d\xi} \left(\frac{\partial q}{\partial \delta} \right) = q_0 \xi$, $\frac{\partial q}{\partial \delta}(0) = 0$. Substituting (2.3) into (2.10) results in the following expression for the leading order splitting distance,

$$\Delta = - \int_{-\infty}^{\infty} \frac{q\xi}{\sqrt{2}} \tanh \left(\frac{\xi}{\sqrt{2}} \right) \operatorname{sech}^2 \left(\frac{\xi}{\sqrt{2}} \right) d\xi = -q_0 \sqrt{2}.$$

Thus, $W^u(\mathcal{M}_\varepsilon^-) \cap W^s(\mathcal{M}_\varepsilon^+) \cap \{u = 0\}$ must be $\mathcal{O}(\varepsilon)$ close to $q = 0$. By the symmetries (2.2), we conclude that $W^u(\mathcal{M}_\varepsilon^-) \cap W^s(\mathcal{M}_\varepsilon^+) \cap \{u = 0\}$ must be identically $q = 0$. Hence, again by (2.2), any solution that connects $\mathcal{M}_\varepsilon^-$ to $\mathcal{M}_\varepsilon^+$ must have a u component that is odd with respect to ξ and a v component that is even with respect to ξ .

We are now ready to determine the take off (touch down) curves $T_o^- \subset \mathcal{M}_\varepsilon^-$ ($T_d^+ \subset \mathcal{M}_\varepsilon^+$) [6, 5]. These curves represent the points at which the one-dimensional family of orbits in $W^u(\mathcal{M}_\varepsilon^-) \cap W^s(\mathcal{M}_\varepsilon^+)$ leave (land on) $\mathcal{M}_\varepsilon^\pm$. Let the elements of this family be denoted $\gamma(\xi; p)$, where the parameter $p > 0$ corresponds to the p -component of $\gamma(\xi; p)$ as it crosses through $\{u = q = 0\}$. Note that the γ -family forms the Fenichel fibering of $W^u(\mathcal{M}_\varepsilon^-) \cap W^s(\mathcal{M}_\varepsilon^+)$ [9] and that each $\gamma(\xi; p)$ is asymptotically close to an unperturbed orbit given in (2.3). To each $\gamma(\xi; p)$ we associate two orbits, $\gamma_{\mathcal{M}_\varepsilon^-}(\xi; p) \subset \mathcal{M}_\varepsilon^-$ and $\gamma_{\mathcal{M}_\varepsilon^+}(\xi; p) \subset \mathcal{M}_\varepsilon^+$ by the fact that $\|\gamma(\xi; p) - \gamma_{\mathcal{M}_\varepsilon^\pm}(\xi; p)\|$ is exponentially small if $\pm\xi > \mathcal{O}(\varepsilon^{-1})$. We define T_o^- and T_d^+ as the collections of base points of the Fenichel fibers on $\mathcal{M}_\varepsilon^-$ and on $\mathcal{M}_\varepsilon^+$,

$$T_o^- = \bigcup_{p>0} \gamma_{\mathcal{M}_\varepsilon^-}(0; p), \quad T_d^+ = \bigcup_{p>0} \gamma_{\mathcal{M}_\varepsilon^+}(0; p). \quad (2.11)$$

We can compute the leading order structure of T_o^- and T_d^+ by considering the effect of the journey through the fast field on the slow variables v and q . Since $v_\xi = \varepsilon q$ and $q = \mathcal{O}(\varepsilon)$ it follows that the change in v through the fast field is of higher order, i.e. $\mathcal{O}(\varepsilon^2)$. By construction, q will be an odd function of ξ , thus the value of q for a given v on T_o^- must be $-\frac{1}{2}\Delta q(v)$, where $\Delta q(v)$ is the change in q due to one full pass through the fast field (during which v remains (at leading order) constant, $v = v_0$). Similarly, the value of q on T_d^+ must be $\frac{1}{2}\Delta q(v)$. Since we already know that both v and q must be $\mathcal{O}(\varepsilon)$ in this regular case, we compute $\Delta q(0)$ (by (2.1), (2.3)),

$$\Delta q(0) = \int_{-\infty}^{\infty} \dot{q}|_{v=0} d\xi, = -\varepsilon \int_{-\infty}^{\infty} \left[1 - \tanh^2 \left(\frac{\xi}{\sqrt{2}} \right) \right] H(\tanh^2 \left(\frac{\xi}{\sqrt{2}} \right), 0) d\xi + \mathcal{O}(\varepsilon^2).$$

To establish the existence of the heteroclinic orbit $\Gamma_h^+(\xi)$, we consider the intersection $T_o^- \cap W^u(-1, 0, 0, 0)|_{\mathcal{M}_\varepsilon^-}$ on $\mathcal{M}_\varepsilon^-$, $\mathcal{O}(\varepsilon)$ close to $(-1, 0, 0, 0)$. Thus, T_o^- and $W^u(-1, 0, 0, 0)|_{\mathcal{M}_\varepsilon^-}$ are given by $\{q = -\frac{1}{2}\Delta q(0) + \mathcal{O}(\varepsilon^2)\}$ and $\{q = \sqrt{-G_1}v + \mathcal{O}(\varepsilon^2)\}$. Figure 2.1 shows the superposition of T_o^- with $W^u(-1, 0, 0, 0)|_{\mathcal{M}_\varepsilon^-}$ and of T_d^+ with $W^s(1, 0, 0, 0)|_{\mathcal{M}_\varepsilon^+}$. The v -coordinate of $T_o^- \cap W^u(-1, 0, 0, 0)|_{\mathcal{M}_\varepsilon^-}$ is given in (2.4). Thus, we have established the existence of an orbit $\Gamma_h^+ \in W^u(\mathcal{M}_\varepsilon^-) \cap W^s(\mathcal{M}_\varepsilon^+)$ that is asymptotic to $(-1, 0, 0, 0) \in \mathcal{M}_\varepsilon^-$. Since Γ_h^+ passes through $\{u = 0, q = 0\}$ during its jump through the fast field, it follows by the symmetries (2.2) that Γ_h^+ is indeed the orbit described in the statement of the Theorem. As was already mentioned, the existence of Γ_h^- also follows immediately from (2.2). \square

REMARK 2.2. We note that if $G_1 = \mathcal{O}(\varepsilon^\sigma)$ for some $\sigma \in [0, 2)$ then the intersection of T_o^- and $W^u(-1, 0, 0, 0)|_{\mathcal{M}_\varepsilon^-}$ will result in a value of v_0 of $\mathcal{O}(\varepsilon^{2-\sigma}) \ll \mathcal{O}(1)$ (2.4), thus $\Gamma_h^+(\xi)$ will still be a regular perturbation of the orbit in the scalar limit. Moreover, this argument also shows that singular orbits may exist for $G_1 = \mathcal{O}(\varepsilon^2)$.

2.2. The super-slow limit: an example. In this section we consider the ‘significant degeneration’ $G_1(\varepsilon) = \mathcal{O}(\varepsilon^2)$. For simplicity, we only consider the case in which the flow on the slow

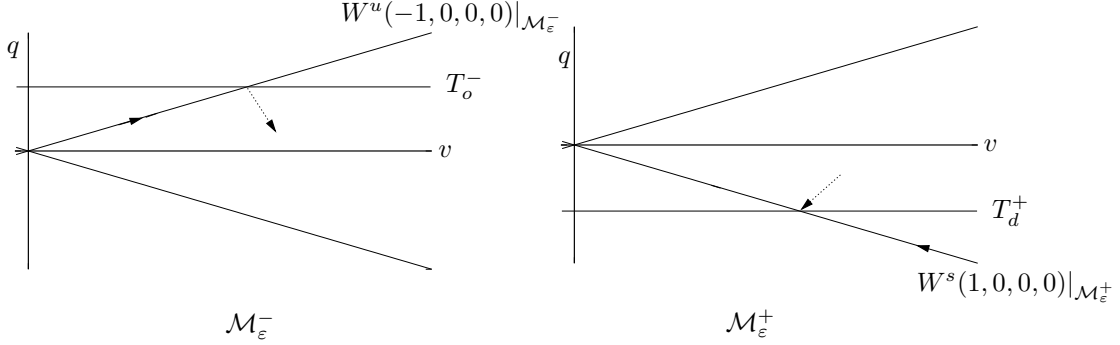


FIG. 2.1. Superposition of the take off and touch down curves $T_{o,d}^\pm$ with $W^{s,u}(\pm 1, 0, 0, 0)|_{\mathcal{M}_\varepsilon^\pm}$. The intersections $T_o^- \cap W^u(-1, 0, 0, 0)|_{\mathcal{M}_\varepsilon^-}$ and $T_d^+ \cap W^s(1, 0, 0, 0)|_{\mathcal{M}_\varepsilon^+}$ determine the heteroclinic front solution $\Gamma_h^+(\xi; \varepsilon)$. The dotted arrows indicates the orbit $\Gamma_h^+(\xi)$ 'taking off' and 'touching down'.

manifolds $\mathcal{M}_\varepsilon^\pm$ is linear, i.e. $G(v; \varepsilon) = \varepsilon^2 G_1(\varepsilon) \stackrel{\text{def}}{=} -\varepsilon^2 \gamma$, where γ does not depend on ε . Moreover, we first consider an explicit expression for $H(u^2, v; \varepsilon)$, $H(u^2, v; \varepsilon) = H_0 u^2$. The case of a general $H(U^2, V)$ will be considered in the next subsection. We refer to Remark 2.4 for a brief discussion of the case of a general function $G(V)$. System (2.1) reduces to

$$\begin{cases} \dot{u} &= p \\ \dot{p} &= -(1 + v - u^2)u \\ \dot{v} &= \varepsilon q \\ \dot{q} &= \varepsilon [-(1 + v - u^2)H_0 u^2 + \varepsilon^2 \gamma v]. \end{cases} \quad (2.12)$$

This system has various types of (singular) heteroclinic orbits.

THEOREM 2.3. *Assume that $G(V) = -\varepsilon^2 \gamma V$, $H(U^2, V) = H_0 U^2$ and that ε is small enough.*
(i): $H_0 > 0$. *If $\gamma > \gamma_{\text{double}}$, where $\gamma_{\text{double}} = \frac{3}{2}H_0^2 + \mathcal{O}(\varepsilon)$, (2.12) has two pairs of heteroclinic orbits, $\Gamma_h^{+,j}(\xi; \varepsilon) = (u_h^j(\xi), p_h^j(\xi), v_h^j(\xi), q_h^j(\xi))$, $j = 1, 2$, and their symmetrical counterparts $\Gamma_h^{-,j}(\xi; \varepsilon) = (-u_h^j(\xi), -p_h^j(\xi), v_h^j(\xi), q_h^j(\xi))$, with $\lim_{\xi \rightarrow \pm\infty} \Gamma_h^{+,j}(\xi; \varepsilon) = (\pm 1, 0, 0, 0)$. In the fast field $u_h^j(\xi)$, respectively $v_h^j(\xi)$, is asymptotically and uniformly close to $u_0(\xi; v_j)$ (2.3) resp. v_j ; the constants v_j are the zeros of $\sqrt{\gamma}v = \frac{2}{3}\sqrt{2}H_0(v+1)^{3/2}$ so that $0 < v_1 < 2 < v_2$ (at leading order). In the slow field, $\Gamma_h^{+,j}(\xi; \varepsilon)$ is exponentially close to $W^{u,s}(\pm 1, 0, 0, 0)|_{\mathcal{M}_\varepsilon^\pm} \subset \mathcal{M}_\varepsilon^\pm$. The orbits $\Gamma_h^{\pm,1}(\xi; \varepsilon)$ and $\Gamma_h^{\pm,2}(\xi; \varepsilon)$ merge in a saddle-node bifurcation of heteroclinic orbits as $\gamma \downarrow \gamma_{\text{double}}$. There are no heteroclinic orbits for $\gamma < \gamma_{\text{double}}$.*

(ii): $H_0 < 0$. *The relation $\sqrt{\gamma}v = \frac{2}{3}\sqrt{2}H_0(v+1)^{3/2}$ has a unique zero for all $\gamma > 0$ and there is one pair of heteroclinic orbits $\Gamma_h^\pm(\xi; \varepsilon)$ for all $\gamma > 0$. These orbits have the same structure as described in (i).*

The orbits $\Gamma_h^{\pm(j)}(\xi; \varepsilon)$ correspond to the front solutions $(U_h^{\pm(j)}(\xi; \varepsilon), V_h^{\pm(j)}(\xi; \varepsilon))$ of (1.6) with $U_h^{\pm(j)}(\xi; \varepsilon) = \pm u_h^j(\xi; \varepsilon)$ odd, and $V_h^{\pm(j)}(\xi; \varepsilon) = v_h^j(\xi; \varepsilon)$ even as function of ξ .

Proof. The essence of the analysis of the super-slow system is similar to that of the regular case. The important difference being that, although the change in q by a 'jump' through the fast field is still $\mathcal{O}(\varepsilon)$, the v -coordinate of the heteroclinic orbit may now be $\mathcal{O}(1)$, due to the super-slow character of the flow on $\mathcal{M}_\varepsilon^\pm$. It is this difference that will cause the bifurcation and the formation of the second orbit in case (i). The flow on the slow manifold is now $\mathcal{O}(\varepsilon^2)$, i.e. super-slow, and is at leading order governed by,

$$v'' = \varepsilon^2 \gamma v. \quad (2.13)$$

Since the right hand side of this equation is $\mathcal{O}(\varepsilon^2)$, one might expect that one needs to incorporate the higher order corrections to the approximation of $\mathcal{M}_\varepsilon^\pm$ (2.8) to determine the leading order flow

on $\mathcal{M}_\varepsilon^\pm$. However, the $\mathcal{O}(\varepsilon^2)$ correction contains a term with a q^2 factor and a term with $G(v)$ (2.8). Since we consider $q = \mathcal{O}(\varepsilon)$ on $\mathcal{M}_\varepsilon^\pm$ and since $G(v) = \mathcal{O}(\varepsilon^2)$, the resulting correction will not be of leading order.

Again the equilibria on $\mathcal{M}_\varepsilon^\pm$ are saddles, with stable and unstable directions, $(\pm 1, \varepsilon\sqrt{\gamma})$. As in Theorem 2.1 we only consider the orbit that jumps from $\mathcal{M}_\varepsilon^-$ to $\mathcal{M}_\varepsilon^+$ (the others follows from the symmetry (2.2)). We repeat the Melnikov calculations and again conclude that, $W^u(\mathcal{M}_\varepsilon^-) \cap W^s(\mathcal{M}_\varepsilon^+) \cap \{u = 0\}$ must be identically $q = 0$. Hence, again by (2.2), any solution that connects $\mathcal{M}_\varepsilon^-$ to $\mathcal{M}_\varepsilon^+$ must have a u component that is odd with respect to ξ and a v component that is even with respect to ξ .

We define the take off, T_o^- , and touch down, T_d^+ , curves as in (2.11). We find the leading order behavior of T_d^+ and T_o^- , by calculating the change in q as we traverse the fast field. As in the regular case, v remains a constant up to $\mathcal{O}(\varepsilon^2)$ and the value of q on the take off (touch down) curve must be $-\frac{1}{2}\Delta q(v_0)$ ($\frac{1}{2}\Delta q(v_0)$), where v_0 is the (leading order) constant value of the v -coordinate of the orbit that is heteroclinic to $\mathcal{M}_\varepsilon^+$ in the fast field. The calculation of the change in q is similar to that of the regular case except that v_0 now effects the leading order term (2.3),

$$\begin{aligned} \Delta q(v_0) &= -\varepsilon H_0(1+v_0)^2 \int_{-\infty}^{\infty} \left[1 - \tanh^2 \left(\sqrt{\frac{v_0+1}{2}} \xi \right) \right] \tanh^2 \left(\sqrt{\frac{v_0+1}{2}} \xi \right) d\xi + \mathcal{O}(\varepsilon^2) \\ &= -\varepsilon \frac{2\sqrt{2}}{3} H_0 (v_0 + 1)^{3/2} + \mathcal{O}(\varepsilon^2). \end{aligned}$$

The heteroclinic orbits are again determined by $T_o^- \cap W^u(-1, 0, 0)|_{\mathcal{M}_\varepsilon^-}$, where $T_o^- = \{q =$

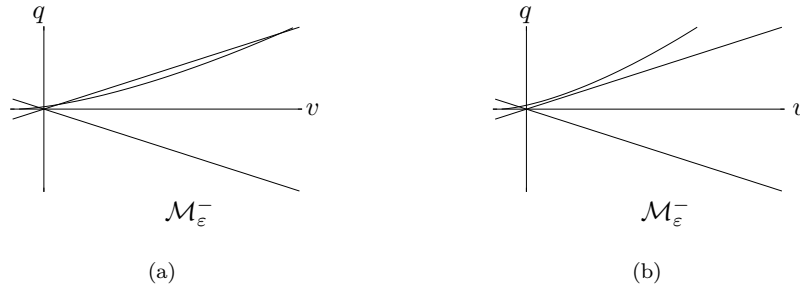


FIG. 2.2. Superposition of T_o^- with $W^u(-1, 0, 0)|_{\mathcal{M}_\varepsilon^-}$ in the super-slow case with $H_0 > 0$, for $\gamma > \gamma_{\text{double}}$ (a) and $\gamma > \gamma_{\text{double}}$ (b).

$-\frac{1}{2}\Delta q(v_0) + \mathcal{O}(\varepsilon^2)\}$ and $W^u(-1, 0, 0)|_{\mathcal{M}_\varepsilon^-} = \{q = \varepsilon\sqrt{\gamma}v + \mathcal{O}(\varepsilon^2)\}$

$$\frac{2\sqrt{2}}{3} H_0 (v_0 + 1)^{3/2} = \sqrt{\gamma} v_0, \quad (2.14)$$

see Figure 2.2. Thus, in the super-slow case, a heteroclinic orbit may leave $\mathcal{M}_\varepsilon^-$ with a v -coordinate of $\mathcal{O}(1)$. Now if $H_0 > 0$ and $\gamma > \gamma_{\text{double}} = \frac{3}{2}H_0^2 + \mathcal{O}(\varepsilon)$, (2.14) has two possible solutions, $v_0 = v_j$, $j = 1, 2$, with $0 < v_1 < 2 < v_2$ (at leading order). These intersection correspond to the heteroclinic orbits $\Gamma_h^{+,j}(\xi)$. For $\gamma < \gamma_{\text{double}}$, there are no solutions to (2.14) and thus no heteroclinic connections exist: the orbits $\Gamma_h^{+,1}(\xi)$ and $\Gamma_h^{+,2}(\xi)$ have coalesced at $\gamma = \gamma_{\text{double}}$. In the case that $H_0 < 0$, (2.14) has a unique solution for all values of $\gamma > 0$, there is only one pair of heteroclinic orbits. \square

REMARK 2.4. If $G(V)$ is not linear in the singular limit (i.e. $G_1 = \mathcal{O}(\varepsilon^2)$), then the analysis becomes more involved, but there are no essentially new phenomena. In this case, the magnitude (w.r.t. ε) of the second derivative of $G(v)$ at $v = 0$ will start to play a role comparable to G_1 . Moreover, the flow on $\mathcal{M}_\varepsilon^\pm$ is nonlinear, so that $W^{u,s}(\pm 1, 0, 0)|_{\mathcal{M}_\varepsilon^\pm}$ is no longer a straight line (at leading order), therefore, many ‘new’ intersections of $T_o^- \cap W^u(-1, 0, 0)|_{\mathcal{M}_\varepsilon^-}$, and thus ‘new’ heteroclinic orbits, may appear.

2.3. The super-slow limit: the general case. We now consider the general super-slow problem, i.e. (2.1) with $G = -\varepsilon^2\gamma v$. The treatment of the general super-slow case and (2.12) is in essence identical to that of the previous section. However, the statement of the main results cannot be formulated as explicit as in Theorem 2.3, as long as there is no explicit expression given for $H(U^2, V)$. Nevertheless, the character of the existence result is similar to that of Theorem 2.3, there can be various kinds of heteroclinic orbits that might coalesce in saddle-node bifurcations.

As in the proofs of Theorems 2.1 and 2.3, the existence of the heteroclinic orbits is established by the intersection of T_o^- and $W^u(-1, 0, 0, 0)|_{\mathcal{M}_\varepsilon^-}$, i.e. by the solution v_0 of

$$\sqrt{\gamma}v_0 = \frac{1}{2} \int_{-\infty}^{\infty} [1 + v_0 - u_0^2(\xi; v_0)] H(u_0^2(\xi; v_0), v_0) d\xi, \quad (2.15)$$

at leading order. Note that the right hand side equals $-\frac{1}{2}\Delta q(v_0)$, i.e. half the accumulated change in q during a circuit through the fast field, and that we have used (2.3).

THEOREM 2.5. *Assume that $G(V) = -\varepsilon^2\gamma V$, and that ε is small enough. System (2.1) has $n \geq 0$ pairs of heteroclinic orbits, $\Gamma_h^{\pm, j}(\xi; \varepsilon) = (\pm u_h^{\pm, j}(\xi), \pm p_h^{\pm, j}(\xi), v_h^{\pm, j}(\xi), q_h^{\pm, j}(\xi))$, where $j = 1, \dots, n$, with $\lim_{\xi \rightarrow \pm\infty} \Gamma_h^{\pm, j}(\xi; \varepsilon) = (\pm 1, 0, 0, 0)$. The number $n = n(\gamma)$ is given by the number of solutions v_j of (2.15). In the fast field $u_h^j(\xi)$, respectively $v_h^j(\xi)$, is asymptotically and uniformly close to $u_0(\xi; v_j)$ (2.3) resp. v_j , where the constant v_j is the j -th zero of (2.15). In the slow field, $\Gamma_h^{\pm, j}(\xi; \varepsilon)$ is exponentially close to $W^{u, s}(\pm 1, 0, 0, 0)|_{\mathcal{M}_\varepsilon^\pm} \subset \mathcal{M}_\varepsilon^\pm$.*

Two orbits $\Gamma_h^{\pm, j}(\xi; \varepsilon)$ and $\Gamma_h^{\pm, j+1}(\xi; \varepsilon)$ coalesce in a saddle-node bifurcation of heteroclinic orbits at a certain value $\gamma = \gamma_{\text{double}}^j$, if the zeroes $v_j \leq v_{j+1}$ of (2.15) merge, i.e. if the intersection $T_o^- \cap W^u(-1, 0, 0, 0)|_{\mathcal{M}_\varepsilon^-}$ is non-transversal.

The orbits $\Gamma_h^{\pm, j}(\xi; \varepsilon)$ correspond to the front solutions $(U_h^{\pm, j}(\xi; \varepsilon), V_h^{\pm, j}(\xi; \varepsilon))$ of (1.6) with $U_h^{\pm, j}(\xi; \varepsilon) = \pm u_h^j(\xi; \varepsilon)$ odd, and $V_h^{\pm, j}(\xi; \varepsilon) = v_h^j(\xi; \varepsilon)$ even as function of ξ .

The proof of this result is in essence identical to that of Theorem 2.3. In Figure 2.3 two examples of the possible richness of the intersection $T_o^- \cap W^u(-1, 0, 0, 0)|_{\mathcal{M}_\varepsilon^-}$ are given.

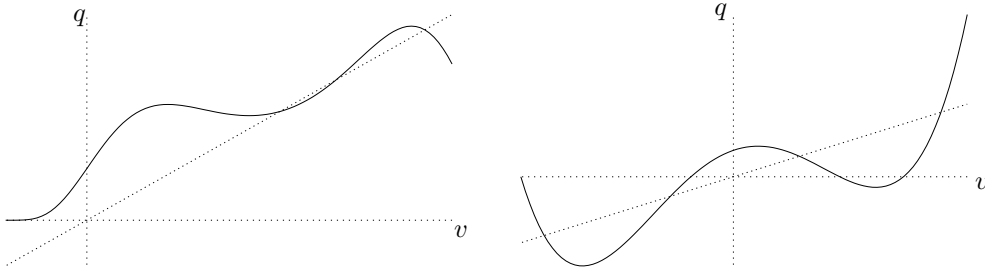


FIG. 2.3. Two examples of the possible character of the intersection $T_o^- \cap W^u(-1, 0, 0, 0)|_{\mathcal{M}_\varepsilon^-}$ for a given $H(U^2, V)$; (a) there are 3 different singular heteroclinic orbits (b) 4 heteroclinic orbits.

3. The stability of fronts. With a slight abuse of notation we (re-)introduce $u(\xi)$ and $v(\xi)$ by

$$U(\xi, t) = U_h(\xi; \varepsilon) + u(\xi)e^{\lambda t}, \quad V(\xi, t) = V_h(\xi; \varepsilon) + v(\xi)e^{\lambda t},$$

substitute this into (1.6), and linearize

$$\begin{aligned} u_{\xi\xi} &+ (1 + V_h - 3U_h^2 - \lambda)u = -U_h v \\ v_{\xi\xi} &= \varepsilon^2 \left\{ 2 \left[H(U_h^2, V_h) - (1 + V_h - U_h^2) \frac{\partial H}{\partial U^2}(U_h^2, V_h) \right] U_h u \right. \\ &\quad \left. - \left[H(U_h^2, V_h) - (1 + V_h - U_h^2) \frac{\partial H}{\partial V}(U_h^2, V_h) + \frac{\partial G}{\partial V}(V_h) - \tau\lambda \right] v \right\}. \end{aligned} \quad (3.1)$$

Note that the front pattern $(U_h(\xi), V_h(\xi))$ corresponds to any of the regular or singular heteroclinic orbits $\Gamma_h^{\pm,j}(\xi)$ of Theorems 2.1, 2.3, 2.5. In the stability analysis of forthcoming sections we will only consider the front patterns of $+$ -type, i.e. those fronts for which $\lim_{\xi \rightarrow \pm\infty} U_h(\xi; \varepsilon) = \pm 1$. Thus, we do not explicitly consider their symmetric counterparts. Due to the symmetry (1.2) this is of course also not necessary. The coupled system of second order equations (3.1) is equivalent to a linear system in \mathbb{C}^4 ,

$$\phi_\xi = A(\xi; \lambda, \varepsilon)\phi \quad \text{with} \quad \phi(\xi) = (u(\xi), p(\xi), v(\xi), q(\xi)), \quad (3.2)$$

where $A(\xi; \lambda, \varepsilon)$ is a 4×4 matrix with $\text{Tr}(A(\xi; \lambda, \varepsilon)) \equiv 0$, and $u_\xi = p$, $v_\xi = \varepsilon q$. It follows that

$$\lim_{\xi \rightarrow \pm\infty} A(\xi; \lambda, \varepsilon) \stackrel{\text{def}}{=} A_\infty^\pm(\lambda, \varepsilon) = \begin{pmatrix} 0 & 1 & 0 & 0 \\ 2 + \lambda & 0 & \mp 1 & 0 \\ 0 & 0 & 0 & \varepsilon \\ \pm 2\varepsilon H_0 & 0 & -\varepsilon(H_0 + G_1 - \tau\lambda) & 0 \end{pmatrix} \quad (3.3)$$

(1.7). The matrices A_∞^\pm have the same set of eigenvalues $\Lambda_i(\lambda, \varepsilon)$, $i = 1, 2, 3, 4$,

$$\Lambda_{1,4}^2(\lambda, \varepsilon) = \lambda + 2 + \mathcal{O}(\varepsilon^2), \quad \Lambda_{2,3}^2(\lambda, \varepsilon) = \varepsilon^2 \frac{\tau\lambda^2 - \lambda(G_1 + H_0 - 2\tau) - 2G_1}{\lambda + 2} + \mathcal{O}(\varepsilon^4). \quad (3.4)$$

Note that both expansions break down as λ approaches -2 (see Remark 3.1). We define a branch cut such that for $z \in \mathbb{C}$ $\arg(\sqrt{z}) \in (-\frac{1}{2}\pi, \frac{1}{2}\pi]$, so that the Λ_i 's can be ordered

$$\text{Re}(\Lambda_4(\lambda, \varepsilon)) < \text{Re}(\Lambda_3(\lambda, \varepsilon)) < 0 < \text{Re}(\Lambda_2(\lambda, \varepsilon)) < \text{Re}(\Lambda_1(\lambda, \varepsilon)) \quad (3.5)$$

This ordering of course breaks down if $\lambda \in \sigma_{\text{ess}}$, the essential spectrum associated to (3.1)/(3.2), since σ_{ess} coincides with values of λ for which either $\text{Re}(\Lambda_{1,4}(\lambda, \varepsilon)) = 0$ or $\text{Re}(\Lambda_{2,3}(\lambda, \varepsilon)) = 0$ [8]; see also section 3.1). The eigenvectors $E_i^\pm(\varepsilon, \lambda)$ of the matrices $A_\infty^\pm(\varepsilon, \lambda)$ associated to $\Lambda_i(\lambda, \varepsilon)$ are given by

$$E_{1,4}^\pm(\varepsilon, \lambda) \begin{pmatrix} 1 \\ \Lambda_{1,4}(\lambda, \varepsilon) \\ \mathcal{O}(\varepsilon^2) \\ \pm \frac{2H_0}{\Lambda_{1,4}(\lambda, \varepsilon)}\varepsilon + \mathcal{O}(\varepsilon^3) \end{pmatrix}, \quad E_{2,3}^\pm(\varepsilon, \lambda) \begin{pmatrix} \pm \frac{1}{\lambda+2} + \mathcal{O}(\varepsilon^2) \\ \mathcal{O}(\varepsilon^2) \\ 1 \\ \frac{1}{\varepsilon}\Lambda_{2,3}(\lambda, \varepsilon) \end{pmatrix} \quad (3.6)$$

(for $\lambda + 2 = \mathcal{O}(1)$ – Remark 3.1).

REMARK 3.1. The expansions (3.4) and (3.6) are only valid for $\lambda + 2 = \mathcal{O}(1)$ with respect to ε . It is straightforward to check that $\Lambda_{1,4}^2(\lambda, \varepsilon) = \mathcal{O}(\varepsilon) = \Lambda_{2,3}^2(\lambda, \varepsilon)$ if $\lambda + 2 = \mathcal{O}(\varepsilon)$ and that in general, when $\lambda + 2 = \mathcal{O}(\varepsilon^\sigma)$ for some $\sigma \in [0, 1]$, $\Lambda_{1,4}^2(\lambda, \varepsilon) = \mathcal{O}(\varepsilon^\sigma)$ and $\Lambda_{2,3}^2(\lambda, \varepsilon) = \mathcal{O}(\varepsilon^{2-\sigma})$. Thus, $\Lambda_{1,4}$ cannot be assumed to be large/fast compared to $\Lambda_{2,3}$ if $\lambda + 2 = \mathcal{O}(\varepsilon)$. Since $\lambda \approx -2$ is way into the stable region, we do not consider this degeneration further and assume throughout this paper that $|\Lambda_{2,3}| \ll |\Lambda_{1,4}|$.

3.1. The essential spectrum. The essential spectrum associated to the stability of the front patterns $(U, V) = (U_h(\xi), V_h(\xi))$ is fully determined by the spectrum of the linear stability problem for the (trivial) background states (at $\pm\infty$) $(U, V) \equiv (\pm 1, 0)$ [8]. Therefore, we introduce $k \in \mathbb{R}$ and $\alpha, \beta, \lambda \in \mathbb{C}$ by

$$U(x, t) = \pm 1 + \alpha e^{ik\xi + \lambda t}, \quad V(x, t) = \beta e^{ik\xi + \lambda t},$$

and substitute this expression into (1.6) (using (1.3)). This yields the matrix equation

$$\begin{pmatrix} -k^2 - 2 & \pm 1 \\ \mp 2\varepsilon^2 H_0 & -k^2 + \varepsilon^2(H_0 + G_1) \end{pmatrix} \begin{pmatrix} \alpha \\ \beta \end{pmatrix} = \lambda \begin{pmatrix} \alpha \\ \varepsilon^2 \tau \beta \end{pmatrix},$$

where G_1 and H_0 have been introduced in (1.7). Thus, $\lambda = \lambda(k^2)$ is a solution of the characteristic equation

$$Q(\lambda, k) = (\lambda + k^2 + 2)(\varepsilon^2 \tau \lambda + k^2 - \varepsilon^2(H_0 + G_1)) + 2\varepsilon^2 H_0 = 0. \quad (3.7)$$

Note that this equation holds for both background states $(\pm 1, 0)$, due to the symmetry (1.2). We may conclude

LEMMA 3.2. *The essential spectrum σ_{ess} associated to (3.1) is given by the solutions $\lambda = \lambda(k^2)$ of (3.7) with $k \in \mathbb{R}$; σ_{ess} is stable, i.e. $\sigma_{\text{ess}} \in \{\text{Re}(\lambda) < 0\}$, if $G_1 < 0$ and $H_0 + G_1 - 2\tau < 0$.*

Proof. The two conditions in this lemma are obtained directly from

$$\begin{aligned} \lambda_1 + \lambda_2 &= \frac{1}{\varepsilon^2 \tau} [\varepsilon^2(H_0 + G_1 - 2\tau) - k^2(1 + \varepsilon^2 \tau)] < 0 \quad \forall k \\ \lambda_1 \lambda_2 &= \frac{1}{\varepsilon^2 \tau} [k^4 + k^2(2 - \varepsilon^2(H_0 + G_1)) - 2\varepsilon^2 G_1] > 0 \quad \forall k. \end{aligned} \quad (3.8)$$

Both relations attain their extremal value at $k = 0$. \square

However, we need to have more information on the essential spectrum than just this stability result. In section 4 we will see that the appearance of edge bifurcations is closely related to the structure of σ_{ess} . We focus on the stable case $G_1 < 0$ and $H_0 + G_1 - 2\tau < 0$. It is straightforward to check that (3.7) has two solution $\lambda_{1,2}(k) \in \mathbb{R}$ for all $k \in \mathbb{R}$ if $H_0 < 0$. As H_0 passes through zero two k -intervals, $(-k^+, -k^-)$ and (k^-, k^+) ($0 < k^- < k^+$) appear in which $\lambda_{1,2}(k)$ are complex valued. These intervals merge (i.e. $k^- \downarrow 0$) as H_0 approaches $(\sqrt{2\tau} - \sqrt{-G_1})^2$. For $(\sqrt{2\tau} - \sqrt{-G_1})^2 < H_0 < 2\tau - G_1$ (which is a non-empty region), $\lambda_{1,2}(k) \in \mathbb{C}$ if $-k^+ < k < k^+$. See Figure 3.1.

3.2. The Evans function. The use of the Evans function in the analysis of linear systems associated to the stability of traveling waves is by now well-established. Here, we give a brief exposition of the characteristics of the Evans function in reaction-diffusion systems. We refer to [1, 17, 10, 4, 5] for the full analytic details of the statements in this section.

We define the complement of the essential spectrum by

$$\mathcal{C}_e = \mathbb{C} \setminus \sigma_{\text{ess}}. \quad (3.9)$$

For $\lambda \in \mathcal{C}_e$ the ordering (3.5) holds, so that

LEMMA 3.3. *For all $\lambda \in \mathcal{C}_e$ there exist two two-dimensional families of solutions $\Phi_-(\xi; \lambda, \varepsilon)$ and $\Phi_+(\xi; \lambda, \varepsilon)$ to (3.2) such that $\lim_{\xi \rightarrow \pm\infty} \phi_{\pm}(\xi; \lambda, \varepsilon) = (0, 0, 0, 0)^t$ for all $\phi_{\pm}(\xi; \lambda, \varepsilon) \in \Phi_{\pm}(\xi; \lambda, \varepsilon)$; $\Phi_{\pm}(\xi; \lambda, \varepsilon)$ depend analytically on λ .*

An eigenfunction of (3.2) must be in the intersection of $\Phi_-(\xi; \lambda, \varepsilon)$ and $\Phi_+(\xi; \lambda, \varepsilon)$. Since $\text{Tr}(A) \equiv 0$, we therefore define the Evans function $\mathcal{D}(\lambda, \varepsilon)$ by

$$\mathcal{D}(\lambda, \varepsilon) = \det[\phi_1(\xi; \lambda, \varepsilon), \phi_2(\xi; \lambda, \varepsilon), \phi_3(\xi; \lambda, \varepsilon), \phi_4(\xi; \lambda, \varepsilon)], \quad (3.10)$$

where $\{\phi_1, \phi_2\}$ (respectively $\{\phi_3, \phi_4\}$) span the space Φ_- (resp. Φ_+). The Evans function is analytic in $\lambda \in \mathcal{C}_e$, its zeroes correspond to eigenvalues of (3.2) counting multiplicities [1, 17]. Of course, this definition does not determine $\mathcal{D}(\lambda)$ uniquely. However, this can be achieved by choosing $\phi_1(\xi)$ and $\phi_2(\xi)$ as follows

LEMMA 3.4. *For all $\lambda \in \mathcal{C}_e$ there is a unique solution $\phi_1(\xi; \lambda, \varepsilon) \in \Phi_-(\xi; \lambda, \varepsilon)$ of (3.2) such that*

$$\lim_{\xi \rightarrow -\infty} \phi_1(\xi; \lambda, \varepsilon) e^{-\Lambda_1(\lambda, \varepsilon)\xi} = E_1^-(\lambda, \varepsilon).$$

(3.4), (3.6). *There exists an analytic transmission function $t_1(\lambda, \varepsilon)$ such that*

$$\lim_{\xi \rightarrow \infty} \phi_1(\xi; \lambda, \varepsilon) e^{-\Lambda_1(\lambda, \varepsilon)\xi} = t_1(\lambda, \varepsilon) E_1^+(\lambda, \varepsilon).$$

For $\lambda \in \mathcal{C}_e$ such that $t_1(\lambda, \varepsilon) \neq 0$ there is a unique solution $\phi_2(\xi; \lambda, \varepsilon) \in \Phi_-(\xi; \lambda, \varepsilon)$ of (3.2), that is independent of $\phi_1(\xi; \lambda, \varepsilon)$, that satisfies

$$\lim_{\xi \rightarrow -\infty} \phi_2(\xi; \lambda, \varepsilon) e^{-\Lambda_2(\lambda, \varepsilon)\xi} = E_2^-(\lambda, \varepsilon) \quad \text{and} \quad \lim_{\xi \rightarrow \infty} \phi_2(\xi; \lambda, \varepsilon) e^{-\Lambda_1(\lambda, \varepsilon)\xi} = (0, 0, 0, 0)^t.$$

There exists a second meromorphic transmission function $t_2(\lambda, \varepsilon)$, that is determined by

$$\lim_{\xi \rightarrow \infty} \phi_2(\xi; \lambda, \varepsilon) e^{-\Lambda_2(\lambda, \varepsilon)\xi} = t_2(\lambda, \varepsilon) E_2^+(\lambda, \varepsilon).$$

The solutions $\phi_{3,4}(\xi; \lambda, \varepsilon) \in \Phi_+(\xi; \lambda, \varepsilon)$ of (3.2) can be defined likewise. Since $\sum_{i=1}^4 \Lambda_i(\lambda, \varepsilon) \equiv 0$ (3.4),

$$\mathcal{D}(\lambda, \varepsilon) = \det[\phi_1(\xi) e^{-\Lambda_1 \xi}, \phi_2(\xi) e^{-\Lambda_2 \xi}, \phi_3(\xi) e^{-\Lambda_3 \xi}, \phi_4(\xi) e^{-\Lambda_4 \xi}],$$

so that $\mathcal{D}(\lambda, \varepsilon)$ can be decomposed into a product of $t_1(\lambda, \varepsilon)$ and $t_2(\lambda, \varepsilon)$ by taking the limit $\xi \rightarrow +\infty$.

LEMMA 3.5. *Let $\lambda \in \mathcal{C}_e$, then*

$$\mathcal{D}(\lambda, \varepsilon) = t_1(\lambda, \varepsilon) t_2(\lambda, \varepsilon) \det [E_1^+(\lambda, \varepsilon), E_2^+(\lambda, \varepsilon), E_3^+(\lambda, \varepsilon), E_4^+(\lambda, \varepsilon)]. \quad (3.11)$$

We conclude that the eigenvalues of (3.2) correspond to zeroes of the transmission functions $t_1(\lambda, \varepsilon)$ and $t_2(\lambda, \varepsilon)$. However, we will see that a zero of $t_1(\lambda, \varepsilon)$ does not necessarily correspond to a zero of $\mathcal{D}(\lambda, \varepsilon)$, since $t_2(\lambda, \varepsilon)$ can have poles (see also [4, 5]).

3.3. The fast eigenvalues. Next section will be devoted to the analysis of (the zeroes of) $t_2(\lambda, \varepsilon)$, here we consider the zeroes of the fast transmission function $t_1(\lambda, \varepsilon)$. In order to do so, we first consider the stability problem associated to the front solution $U_f(\xi; V_0)$, with $U_f(\xi; V_0) \rightarrow \pm(1 + V_0)$ as $\xi \rightarrow \pm\infty$, of the scalar fast reduced limit problem (1.5),

$$w_{\xi\xi} + (1 + V_0 - 3u_0^2(\xi; V_0) - \lambda)w = 0, \quad (3.12)$$

since $U_f(\xi; V_0) = u_0(\xi; V_0)$ (2.3). This system can be written as a linear system in \mathbb{C}^2 ,

$$\psi_{\xi} = B(\xi; \lambda)\psi \quad \text{with} \quad \psi(\xi) = (u(\xi), p(\xi)), \quad (3.13)$$

where $B(\xi; \lambda)$ is a 2×2 matrix of which the coefficients are by construction $\mathcal{O}(\varepsilon)$ close (uniformly in ξ) to those of the 2×2 block in the upper left corner of the 4×4 matrix $A^{\pm}(\xi; \lambda, \varepsilon)$ defined in (3.2), if we set $V_0 = V_h(0)$. The Evans function associated to this problem can be written as $\mathcal{D}_f(\lambda) = \det[\psi_1(\xi, \lambda), \psi_4(\xi, \lambda)]$, in which $\psi_1(\xi)$ and $\psi_4(\xi)$ are solutions of (3.2) determined by $\lim_{\xi \rightarrow -\infty} \psi_1(\xi) e^{-\sqrt{\lambda+2}\xi} = (1, \sqrt{\lambda+2})^t$ and $\lim_{\xi \rightarrow \infty} \psi_4(\xi) e^{\sqrt{\lambda+2}\xi} = (1, -\sqrt{\lambda+2})^t$ (where $\pm\sqrt{\lambda+2}$ and $(1, \pm\sqrt{\lambda+2})^t$ are the eigenvalues and eigenvectors of the matrix $B_{\infty}(\lambda) = \lim_{\xi \rightarrow \pm\infty} B(\xi; \lambda)$ (compare to (3.4), (3.6))). As for the full system, we can define an analytic fast reduced transmission function $t_f(\lambda)$ by $\lim_{\xi \rightarrow \infty} \psi_1(\xi) e^{-\sqrt{\lambda+2}\xi} = t_f(\lambda)(1, \sqrt{\lambda+2})^t$, so that

$$\mathcal{D}_f(\lambda) = \lim_{\xi \rightarrow \infty} \det[\psi_1(\xi), \psi_4(\xi)] = \det[t_f(\lambda)(1, \sqrt{\lambda+2})^t, (1, -\sqrt{\lambda+2})^t] = -2t_f(\lambda)\sqrt{\lambda+2}.$$

The transmission function $t_1(\lambda)$ is, by construction, asymptotically close to its fast reduced limit $t_f(\lambda)$.

LEMMA 3.6. *Let $\lambda_i^f \in \mathcal{C}_e$ such that $t_f(\lambda_i^f) = 0$. There is a uniquely determined $\lambda_i(\varepsilon)$ with $\lim_{\varepsilon \rightarrow 0} \lambda_i(\varepsilon) = \lambda_i^f$ such that $t_1(\lambda_i(\varepsilon), \varepsilon) = 0$; $t_1(\lambda, \varepsilon) \neq 0$ for $\lambda \neq \lambda_i(\varepsilon)$.*

The proof of this Lemma is completely analogous to the proofs of similar statements in [1, 10, 4, 5]. Hence, we find (the leading order behavior of) the zeroes of $t_1(\lambda, \varepsilon)$ by computing the spectrum of (3.12). By (2.3) and by introducing $\eta = \sqrt{\frac{1}{2}(1 + V_0)}$ we can write (3.12) as

$$w_{\eta\eta} + \left(\frac{6}{\cosh^2 \eta} - P^2 \right) w = 0 \quad \text{with} \quad P^2 = \frac{2\lambda}{1 + V_0} + 4,$$

which is a well-studied problem of Schrödinger/Sturm-Liouville type (see for instance [20, 5]). It has discrete spectrum at $P = 1$ and $P = 4$ and essential spectrum for $P \in i\mathbb{R}$. We conclude that the eigenvalues of (3.12), and thus the leading order approximations of the zeroes of $t_1(\lambda)$, are given by

$$\lambda_1^f = 0, \quad \lambda_2^f = -\frac{3}{2}(1 + V_0) < 0. \quad (3.14)$$

The essential spectrum of (3.12) is given by

$$\sigma_{\text{ess}}^f = \{\lambda \leq -2(1 + V_0)\}. \quad (3.15)$$

We conclude this subsection by stating two simple, but useful results:

LEMMA 3.7. *Let $(u(\xi; \varepsilon), v(\xi; \varepsilon))$ be a pair of eigenfunction solutions of (3.1) associated to a simple eigenvalue $\lambda(\varepsilon)$, then either $u(\xi)$ is even as function of ξ and $v(\xi)$ odd, or $u(\xi)$ is odd and $v(\xi)$ even.*

Proof. We write (3.1) in the following way,

$$v_{\xi\xi} = \varepsilon^2[F_o(\xi)u + F_e(\xi)v]. \quad (3.16)$$

By construction, U_h is an odd function of ξ and V_h is an even function of ξ . It thus follows that the above functions, F_o and F_e must be odd and even functions of ξ respectively. Let (u, v) be an eigenfunctions associated to the eigenvalue λ . We decompose (u, v) into odd and even components, $u = u_o + u_e$, $v = v_o + v_e$, where u_o, v_o are odd and u_e, v_e are even. By the parity of the functions U_h, V_h, F_o and F_e it is clear that (u_o, v_e) and (u_e, v_o) form two independent solutions of the eigenvalue problem associated to the eigenvalue λ . Since we have assumed that λ is simple, we have a contradiction. \square

LEMMA 3.8. *Assume that the eigenfunction solution $v(\xi)$ of (3.1) with eigenvalue $\lambda(\varepsilon)$ is odd, then $\lambda(\varepsilon) \equiv 0$, so that $(u(\xi), v(\xi)) = (U_{h,\xi}(\xi; \varepsilon), V_{h,\xi}(\xi; \varepsilon))$.*

We will see in section 4 that there can be several eigenvalues for which $u(\xi)$ is odd and $v(\xi)$ even.

Proof. It is clear that there is an eigenvalue $\lambda = 0$ associated to the derivative of the front $(u(\xi), v(\xi)) = (U_{h,\xi}(\xi; \varepsilon), V_{h,\xi}(\xi; \varepsilon))$. We assume there is another eigenfunction with v odd. Since $v_{\xi\xi}$ is $\mathcal{O}(\varepsilon^2)$ and v is odd, it follows that $|v| \ll 1$ on the fast spatial scale. Hence, the equation for the u -component is to leading order homogeneous and given by (3.12) (with u replaced by w). Lemma 3.7 implies that u is even. Since the only even eigenfunction of (3.12) is $U_{h,\xi}$ with eigenvalue 0, it follows that the leading order behavior of u is given by $U_{h,\xi}$ and that λ is asymptotically close to 0. We thus write,

$$u = U_{h,\xi} + \delta(\varepsilon)u_1, \quad v = \delta(\varepsilon)v_1, \quad \lambda = \delta(\varepsilon)\hat{\lambda}(\varepsilon), \quad (3.17)$$

where $\delta(\varepsilon) \rightarrow 0$ as $\varepsilon \rightarrow 0$ and $\hat{\lambda}(0) \neq 0$ (i.e. $\delta(\varepsilon)$ represents the leading order magnitude of $\hat{\lambda}$). We substitute (3.17) into (3.1), to get the following equation for u_1 ,

$$u_{1,\xi\xi} + (1 - 3U_h^2)u_1 = \hat{\lambda}U_{h,\xi} - U_hv_1.$$

This equation has the solvability condition, $\int_{-\infty}^{\infty} (\hat{\lambda}U_{h,\xi} - U_hv_1)U_{h,\xi} dy = 0$. Now, v_1 and U_h are odd while $U_{h,\xi}$ is even, thus we have that $\hat{\lambda} = 0$, contradicting our assumption. So the only possible eigenfunctions with v odd must correspond to a 0 eigenvalue and hence, $(u, v) = (U_{h,\xi}, V_{h,\xi})$. \square

4. Slow-fast eigenvalues and edge bifurcations. The ‘slow-fast eigenvalues’ are the eigenvalues that exist due to the interaction of the fast U -equation and the slow V -equation in (1.6), thus, these eigenvalues do not have a counterpart in the fast reduced scalar limit problem (1.5). The slow-fast eigenvalues correspond to the zeroes of the $t_2(\lambda; \varepsilon)$, since this transmission function is based on a balance between slow and fast effects. See also Remark 4.5.

In order to study the combined effect of slow and fast terms, we need to define the region in which the fast ξ -jump takes place more accurately

$$I_f = \left\{ \xi \in \left(-\frac{1}{\sqrt{\varepsilon}}, \frac{1}{\sqrt{\varepsilon}} \right) \right\} \text{ or } \{x \in (-\sqrt{\varepsilon}, \sqrt{\varepsilon})\} \quad (4.1)$$

(1.3). Note that the exact choice of the boundaries of I_f is not relevant, any choice will be suitable as long as it is in the transition zone between x and ξ (i.e. on the boundary of I_f we must have $|x| \ll 1$ and $|\xi| \gg 1$).

4.1. The regular case. Again, we first consider the case $G_1 = \mathcal{O}(1)$ (1.7). In the slow coordinate x (1.3), i.e. outside the region I_f , the equation for u reads

$$(1 - 3U_h^2 - \lambda + \mathcal{O}(\varepsilon))u = -U_h v + \mathcal{O}(\varepsilon^2 u_{xx}) \quad (4.2)$$

(3.1), since $V_h(\xi) = \mathcal{O}(\varepsilon)$ on \mathbb{R} (Theorem 2.1). Thus, u can be expressed in terms of v outside the fast ξ -region I_f (4.1). Using that $U_h^2(\xi; \varepsilon) = 1 + \mathcal{O}(\varepsilon)$ outside I_f (Theorem 2.1), we find for the v -equation of (3.1) on the slow x -scale,

$$\begin{aligned} v_{xx} &= \left[2H(1, 0)U_h + \mathcal{O}(\varepsilon) \right] u - \left[H(1, 0) + \frac{\partial G}{\partial V}(0) - \tau\lambda + \mathcal{O}(\varepsilon) \right] v \\ &= \left[\frac{2H_0}{\lambda+2} - H_0 - G_1 + \tau\lambda + \mathcal{O}(\varepsilon) \right] v + \mathcal{O}(\varepsilon^2 v_{xx}) \end{aligned}$$

(1.7). Hence, outside I_f

$$v_{xx} = \left[\frac{-H_0\lambda + \lambda(\lambda+2)\tau - G_1(\lambda+2)}{\lambda+2} + \mathcal{O}(\varepsilon) \right] v, \quad (4.3)$$

uniformly in ξ . The v -equation is thus at leading order of constant coefficients type. By (3.7) and (3.4) we have on the ξ -scale

$$v_{\xi\xi} = \left[\frac{Q(\lambda; 0)}{\lambda+2} + \mathcal{O}(\varepsilon^3) \right] v = [\Lambda_{2,3}^2(\lambda, \varepsilon) + \mathcal{O}(\varepsilon^3)] v, \quad (4.4)$$

In order to determine an expression for $t_2(\lambda, \varepsilon)$, we need to control the solution $\phi_2(\xi; \lambda, \varepsilon)$ (Lemma 3.4) of (3.2). This is done in the following Lemma.

LEMMA 4.1. *For all $\lambda \in \mathcal{C}_e$ such that $t_1(\lambda, \varepsilon) \neq 0$ there exist $\mathcal{O}(1)$ constants $C_-, C_+ > 0$ and a third meromorphic transmission function $t_3(\lambda, \varepsilon)$ such that*

$$\phi_2(\xi; \lambda, \varepsilon) = \begin{cases} [E_2^-(\lambda) + \mathcal{O}(\varepsilon)] e^{\Lambda_2(\lambda)\xi} + \mathcal{O}(e^{C_-\xi}) & \text{for } \xi < -\frac{1}{\sqrt{\varepsilon}} \\ t_2(\lambda)E_2^+(\lambda)e^{\Lambda_2(\lambda)\xi} + t_3(\lambda)E_3^+(\lambda)e^{\Lambda_3(\lambda)\xi} + \mathcal{O}(e^{-C_+\xi}) & \text{for } \xi > \frac{1}{\sqrt{\varepsilon}}. \end{cases} \quad (4.5)$$

Moreover, there exists an $\mathcal{O}(1)$ constant C_f such that $\|\phi_2(\xi)\| \leq C_f$ for $\xi \in I_f$. The v -coordinate of $\phi_2(\xi)$ satisfies $v(\xi) = 1 + \mathcal{O}(\sqrt{\varepsilon})$ on I_f , so that

$$t_2(\lambda, \varepsilon) + t_3(\lambda, \varepsilon) = 1 + \mathcal{O}(\sqrt{\varepsilon}). \quad (4.6)$$

Proof. The behavior of $\phi_2(\xi)$ outside I_f is determined by (4.4) and (4.2). The approximation (4.5) for $\xi < -1/\sqrt{\varepsilon}$ follows from the definition of $\phi_2(\xi)$ (Lemma 3.4). This same Lemma establishes the leading order term in (4.5) for $\xi \rightarrow \infty$. The transmission function $t_3(\lambda, \varepsilon)$ measures the

component of $\phi_2(\xi)$ that decays on the slow spatial scale x . Inside I_f , $v_{\xi\xi} = \mathcal{O}(\varepsilon^2)$ (3.1) and $\Lambda_{2,3}^2(\lambda, \varepsilon) = \mathcal{O}(\varepsilon^2)$ (3.4), so that (4.6) follows. As in section 3.2 we refrain from giving the full analytic details of this result, since these are essentially the same as in [10, 4, 5]. \square

The transmission function $t_2(\lambda, \varepsilon)$ can be determined by the methods originally developed in [3]. We deduce from Lemma 4.1 that the total change in v_ξ over I_f is given by

$$\Delta_{\text{slow}} v_\xi = 2\varepsilon(t_2(\lambda) - 1)\sqrt{\frac{Q(\lambda; 0)}{\lambda + 2}} + \mathcal{O}(\varepsilon\sqrt{\varepsilon}). \quad (4.7)$$

This change in v_ξ must be an effect of the evolution on the fast ξ -scale, that is given by

$$\Delta_{\text{fast}} v_\xi = \int_{-\frac{1}{\sqrt{\varepsilon}}}^{\frac{1}{\sqrt{\varepsilon}}} v_{\xi\xi}|_{\{u=u_{\text{in}}, v=1\}} d\xi + \mathcal{O}(\varepsilon^2\sqrt{\varepsilon}), \quad (4.8)$$

where $u_{\text{in}}(\xi)$ is a bounded solution of the inhomogeneous problem

$$u_{\xi\xi} + (1 - 3U_h^2(\xi; 0) - \lambda)u = -U_h(\xi; 0) \quad (4.9)$$

(recall that $v(\xi) = 1 + \mathcal{O}(\sqrt{\varepsilon})$ in I_f). The transmission function $t_2(\lambda; \varepsilon)$ is determined by combining (4.7) and (4.8). Since, a priori $\Delta_{\text{slow}} v_\xi = \mathcal{O}(\varepsilon)$ and $\Delta_{\text{fast}} v_\xi = \mathcal{O}(\varepsilon\sqrt{\varepsilon})$ we are led to the following conclusion.

LEMMA 4.2. *Consider $\lambda \in \mathcal{C}_e \cap \{\text{Re}(\lambda) > -2 + \delta\}$ for some $\delta > 0$ independent of ε . Let $\lambda_2^f = -\frac{3}{2}$ be the second eigenvalue of the limit system (3.12) with $V_0 = 0$ (3.14), and let $\lambda^+(0)$ and $\lambda^-(0)$ be the solutions of $Q(\lambda, 0) = 0$ (3.7). Then, $t_2(\lambda) = 1 + \mathcal{O}(\sqrt{\varepsilon})$ if $|\lambda - \lambda_2^f|, |\lambda - \lambda^+(0)|, |\lambda - \lambda^-(0)| = \mathcal{O}(1)$; $t_2(\lambda) = 1 + \mathcal{O}(\varepsilon^{\frac{1}{2}-\sigma})$ if $|\lambda - \lambda_2^f| = \mathcal{O}(\varepsilon^\sigma)$, $|\lambda - \lambda^+(0)| = \mathcal{O}(\varepsilon^{2\sigma})$, or $|\lambda - \lambda^-(0)| = \mathcal{O}(\varepsilon^{2\sigma})$ for some $\sigma \in (0, \frac{1}{2})$.*

Thus, this Lemma establishes that $t_2(\lambda, \varepsilon)$ can only be zero in $\{\text{Re}(\lambda) > -2\}$ if $\lambda \in \mathcal{C}_e$ is $\mathcal{O}(\sqrt{\varepsilon})$ close to λ_2^f or $\mathcal{O}(\varepsilon)$ close to $\lambda^+(0)$ or $\lambda^-(0)$, so we only have to study λ near these 3 points to determine the slow-fast eigenvalues of (3.2). Note that the fast reduced (scalar) limit problem has an eigenvalue $\lambda_2^f = -\frac{3}{2}$ ((3.14), since $V_0 = V_h(0) \rightarrow 0$ as $\varepsilon \rightarrow 0$ (Theorem 2.1)). We will prove below that $t_2(\lambda)$ has a (simple) zero close to λ_2^f , i.e. that the fast reduced eigenvalue λ_2^f persists.

However, before going further into the details of the (possible) existence of eigenvalues near λ_2^f , $\lambda^+(0)$ or $\lambda^-(0)$, we formulate a result that is an immediate consequence of Lemma 4.2 and that establishes the stability of the wave for values of G_1 and H_0 such that the essential spectrum, and hence $\lambda^+(0)$ and $\lambda^-(0)$, is in the negative half-plane and not too close to the imaginary axis (see Lemma 3.2).

THEOREM 4.3. *Let $\varepsilon > 0$ be small enough and let $G_1 < 0$ and $H_0 + G_1 - 2\tau < 0$ be such that $|G_1|, |H_0 + G_1 - 2\tau| \gg \varepsilon$. The spectrum of the eigenvalue problem (3.1) associated to the stability of the solution $(U_h(\xi; \varepsilon), V_h(\xi; \varepsilon))$ consists of a (unique) eigenvalue at $\lambda = 0$ and a part that is embedded in the region $\{\text{Re}(\lambda) < -\varepsilon\}$. Therefore, $(U_h(\xi; \varepsilon), V_h(\xi; \varepsilon))$ is (spectrally) stable. Note that the operator defined by (3.1) is clearly sectorial in this case (see section 3.1), so that the nonlinear stability of $(U_h(\xi; \varepsilon), V_h(\xi; \varepsilon))$ follows by standard arguments (see for instance [8]).*

Proof of Lemma 4.2. We first note that indeed $\Delta_{\text{fast}} v_\xi = \mathcal{O}(\varepsilon\sqrt{\varepsilon})$ and $\Delta_{\text{slow}} v_\xi = \mathcal{O}(\varepsilon)$, and thus $t_2(\lambda) = 1 + \mathcal{O}(\sqrt{\varepsilon})$, for $\lambda \in \mathcal{C}_e$ that are not asymptotically close to the possible degenerations of (4.8) and (4.7).

The inhomogeneous function u_{in} may become unbounded as λ approaches an eigenvalue, $\lambda_1^f = 0$ or $\lambda_2^f = -\frac{3}{2}$, or the essential spectrum σ_{ess}^f (3.15) of the linear problem associated to the fast reduced limit (3.12) with $V_0 = 0$. To avoid irrelevant technicalities near σ_{ess}^f we assume that $\lambda \in \mathcal{C}_e \cap \{\text{Re}(\lambda) > -2 + \delta\}$. The eigenfunction associated to λ_1^f , i.e. $U_{h,\xi}(\xi; 0)$ is odd, which implies that the inhomogeneous (and even) term $U_h(\xi; 0)$ satisfies the solvability condition associated to (4.9) at $\lambda = 0$. Hence, u_{in} remains bounded as $\lambda \rightarrow 0$, so that $t_2(\lambda) = 1 + \mathcal{O}(\sqrt{\varepsilon})$ also near $\lambda = 0$

[4, 5]. The eigenfunction associated to λ_2^f is even, thus u_{in} grows as $1/(\lambda_2^f - \lambda)$ as $\lambda \rightarrow \lambda_2^f$ [20, 4, 5], which implies that $t_2(\lambda, \varepsilon) - 1 = \mathcal{O}(\varepsilon^{\frac{1}{2}-\sigma})$ if $|\lambda - \lambda_2^f| = \mathcal{O}(\varepsilon^\sigma)$ for some $\sigma \in (0, \frac{1}{2})$.

The behavior of $t_2(\lambda)$ near the degenerations of (4.7), i.e. the zeroes $\lambda^\pm(0)$ of $Q(\lambda; 0)$, follows from observing that $\Delta_{\text{slow}} v_\xi = (t_2 - 1) \times \mathcal{O}(\varepsilon^{1+\sigma})$ if λ is $\mathcal{O}(\varepsilon^{2\sigma})$ close to $\lambda^+(0)$ or to $\lambda^-(0)$ for some $\sigma \in (0, \frac{1}{2})$. \square

It now follows, by a (standard) winding number argument [1, 4, 5], that the eigenvalue λ_2^f persists as an eigenvalue of the full system (3.1) if it is not embedded in the essential spectrum.

LEMMA 4.4. *Let G_1 and H_0 be such that σ_{ess} does not intersect an $\mathcal{O}(\varepsilon^\sigma)$ neighborhood of λ_2^f , for some $\sigma < \frac{1}{2}$. Then, there is an eigenvalue $\lambda_2(\varepsilon)$ of (3.1) with $\lim_{\varepsilon \rightarrow 0} \lambda_2(\varepsilon) = \lambda_2^f = -\frac{3}{2}$.*

Proof. By the assumptions in the Lemma, there exists a contour K in the complex λ -plane that does not intersect σ_{ess} , that encircles an $\mathcal{O}(\varepsilon^\sigma)$ neighborhood of λ_2^f and that is $\mathcal{O}(\varepsilon^\sigma)$ close to λ_2^f . It follows from Lemma 4.2 that $t_2(\lambda) = 1 + \mathcal{O}(\varepsilon^{\frac{1}{2}-\sigma})$ for $\lambda \in K$, thus, the winding number of $t_2(\lambda)$ over K is 0. However, $t_2(\lambda)$ must have a (simple) pole in the interior of K – as is observed in the proof of Lemma 4.2. We conclude that $t_2(\lambda)$ must also have a (simple, real) eigenvalue in the interior of K . \square

The possible existence of slow-fast eigenvalues near $\lambda^+(0)$ or $\lambda^-(0)$ is much more subtle. Since such eigenvalues only become relevant to the stability of the solution $(U_h(\xi; \varepsilon), V_h(\xi; \varepsilon))$ as G_1 (or $H_0 + G_1 - 2\tau$) approaches 0 (Theorem 4.3) we will consider this issue in the forthcoming sections.

REMARK 4.5. The eigenvalues $\lambda_1(\varepsilon) = 0$ and $\lambda_2(\varepsilon) \rightarrow -\frac{3}{2}$ as $\varepsilon \rightarrow 0$ can be interpreted as ‘fast’ eigenvalues, since they correspond to eigenvalues of the fast reduced limit problem. However, strictly speaking both eigenvalues also have the slow-fast structure described in the beginning of this section.

First, we of course know that $\lambda_1(\varepsilon) = 0$ is an eigenvalue – see also Lemma 3.8. Thus it is a zero of $\mathcal{D}(\lambda, \varepsilon)$. Since $t_2(\lambda) = 1 + \mathcal{O}(\sqrt{\varepsilon})$ for λ near 0, see the proof of Lemma 4.2, we conclude that $t_1(0; \varepsilon) \equiv 0$ (note that this in a sense obvious result does not follow directly from Lemma 3.6). Thus, the solution $\phi_1(\xi; 0, \varepsilon)$ of (3.2) that by construction has a purely fast structure for $\xi \ll -1$, does not blow up as $e^{\Lambda_1(0, \varepsilon)\xi}$ as $\xi \rightarrow \infty$ (Lemma 3.4). Nevertheless, the eigenfunction associated to $\lambda = 0$, $(U_{h, \xi}(\xi), V_{h, \xi}(\xi))$ has a clear slow-fast structure, that it inherits from $(U_h(\xi), V_h(\xi))$ (Theorem 2.1). Hence, $\phi_1(\xi; 0, \varepsilon)$ is not the eigenfunction associated to $\lambda = 0$. Neither is $\phi_2(\xi; 0, \varepsilon)$, since $t_2(0) \neq 0$. It follows that the eigenfunction associated to $\lambda = 0$ must be a linear combination of $\phi_1(\xi; 0, \varepsilon)$ and $\phi_2(\xi; 0, \varepsilon)$, and thus that $\phi_1(\xi; 0, \varepsilon)$ does not decay as $\xi \rightarrow \infty$, but instead grows linearly (and slowly), as $e^{\Lambda_2(0, \varepsilon)\xi}$ (like $\phi_2(\xi; 0, \varepsilon)$). The linear combination is such that the two growth terms $e^{\Lambda_2(0, \varepsilon)\xi}$ (for $\xi \rightarrow \infty$) cancel.

Second, $\lambda_2(\varepsilon)$ is not a zero of $t_1(\lambda)$, although it is asymptotically close to such a zero, but it is a zero of $t_2(\lambda)$. Thus, $\phi_2(\xi; \lambda_2(\varepsilon), \varepsilon)$ is the eigenfunction of (3.2) at $\lambda = \lambda_2(\varepsilon)$ (and $\phi_1(\xi; \lambda_2(\varepsilon), \varepsilon)$ blows up fast, as $e^{\Lambda_1(\lambda_2(\varepsilon), \varepsilon)\xi}$).

4.2. The super-slow case: an example. In the previous section we have seen that the front might destabilize as G_1 approaches 0 (if we assume that $H_0 + G_1 - 2\tau < 0$). In this case, Theorem 2.1 can no longer be used to establish the existence of the front $(U_h(\xi), V_h(\xi))$. Thus, the question about the stability of the front is closely related to the characteristics of the existence problem (as is usual in the analysis of (traveling) waves, see also [13]). In this section we consider the bifurcation as G_1 approaches 0. Therefore, we assume that $H_0 - 2\tau < 0$ and $\mathcal{O}(1)$ with respect to ε . As in section 2 we consider in the super-slow case the simplified system in which the general function $G(V)$ is replaced by a linear expression: $G(V) = G_1 V = -\varepsilon^2 \gamma V$ (see Remark 2.4). Note that Theorem 4.3 a priori predicts a possible destabilization as G_1 becomes $\mathcal{O}(\varepsilon)$, i.e. already before $G_1 = -\gamma\varepsilon^2$, but it will be shown in the next section that the estimate in Theorem 4.3 is not sharp, in the sense that a bifurcation only occurs as G_1 decreases to $\mathcal{O}(\varepsilon^2)$.

One of the main differences between the analysis in this section and that of the regular case, is the fact that $V_h(\xi)$ is no longer $\mathcal{O}(\varepsilon)$, i.e. $V_h(\xi)$ does not only contribute to the higher order terms in the stability analysis of the front solutions. Nevertheless, we follow the approach of the

previous section and express the solution u of (3.1) in terms of v , outside I_f (see (4.2)),

$$u = -\frac{U_h}{1 + V_h - 3U_h^2 - \lambda}v + \mathcal{O}(\varepsilon^2 u_{xx}) = \left[\frac{U_h}{2(1 + V_h) + \lambda} + \mathcal{O}(\varepsilon^4) \right] v + \mathcal{O}(\varepsilon^2 v_{xx}) \quad (4.10)$$

since $1 + V_h(\xi; \varepsilon) - U_h^2(\xi; \varepsilon) = \mathcal{O}(\varepsilon^4)$ (see (2.8), recall that q^2 and G are $\mathcal{O}(\varepsilon^2)$ in the super-slow case). This yields that

$$\begin{aligned} v_{xx} &= \{2 [H(U_h^2, V_h) + \mathcal{O}(\varepsilon^4)] U_h u - [H(U_h^2, V_h) + \mathcal{O}(\varepsilon^4) - \varepsilon^2 \gamma - \tau \lambda] v\} \\ &= \left\{ \frac{2H(U_h^2, V_h)U_h^2}{2(1+V_h)+\lambda} - H(U_h^2, V_h) + \tau \lambda + \varepsilon^2 \gamma + \mathcal{O}(\varepsilon^4) \right\} v + \mathcal{O}(\varepsilon^2 v_{xx}) \\ &= \left\{ \lambda \left[\tau - \frac{H(1+V_h, V_h)}{2(1+V_h)+\lambda} \right] + \varepsilon^2 \gamma + \mathcal{O}(\varepsilon^4) \right\} v + \mathcal{O}(\varepsilon^2 v_{xx}). \end{aligned} \quad (4.11)$$

It follows from section 3.1 that one of the ‘tips’ of σ_{ess} , $\lambda^+(0)$, is $\mathcal{O}(\varepsilon^2)$ if $G_1 = \mathcal{O}(\varepsilon^2)$ (and $H_0 - 2\tau < 0$), while the other one, $\lambda^-(0)$, is $\mathcal{O}(1)$ and negative (3.8). Thus, the destabilization of the front will either be caused by σ_{ess} at $G_1 = 0 = \gamma$, or possibly by a slow-fast eigenvalue λ that is close to $\lambda^+(0)$ (Lemma 4.2). Therefore, we introduce $\tilde{\lambda}$ by

$$\lambda = \varepsilon^2 \tilde{\lambda}, \quad (4.12)$$

which implies that (4.11) can also be written as a super-slow system,

$$v_{xx} = \varepsilon^2 \left\{ \tilde{\lambda} \left[\tau - \frac{H(1 + V_h, V_h)}{2(1 + V_h)} \right] + \gamma + \mathcal{O}(\varepsilon^2) \right\} v. \quad (4.13)$$

As in section 2.2, we first consider the explicit example in which $H(U^2, V) = H_0 U^2$. Thus, the existence of (several kinds of) front solutions is established by Theorem 2.3. In this case, the equation for v is, on the ξ -scale, given by

$$v_{\xi\xi} = \varepsilon^4 \left[\tilde{\lambda} \left(\tau - \frac{1}{2} H_0 \right) + \gamma + \mathcal{O}(\varepsilon^2) \right] v = [\Lambda_{2,3}^2(\lambda, \varepsilon) + \mathcal{O}(\varepsilon^6)] v, \quad (4.14)$$

see (3.4). Note that this equation is of constant coefficients type, and, at leading order, the same as in the equation for $v_{\xi\xi}$ in the regular case (4.4). Hence, we can copy the arguments leading to Lemma 4.1 and conclude that the fundamental solution $\phi_2(\xi; \varepsilon^2 \tilde{\lambda}, \varepsilon)$ of (3.2) can again be expressed as in (4.5) outside the region I_f . Moreover, as in Lemma 4.1, we may conclude that $t_2(\tilde{\lambda}, \varepsilon) + t_3(\tilde{\lambda}, \varepsilon) = 1 + \mathcal{O}(\sqrt{\varepsilon})$ (4.6).

We may now proceed as in the preceding section (and as in [4, 5]) and determine $t_2(\tilde{\lambda})$ by measuring the change in the $q = v_\xi$ -coordinate of $\phi_2(\xi)$ over the fast field. It follows from (4.14) that

$$\Delta_{\text{slow}} v_\xi = 2\varepsilon^2 (t_2(\tilde{\lambda}) - 1) \sqrt{\tilde{\lambda} \left(\tau - \frac{1}{2} H_0 \right) + \gamma + \mathcal{O}(\varepsilon^2 \sqrt{\varepsilon})}. \quad (4.15)$$

Note that we have to assume that $\tilde{\lambda} \left(\tau - \frac{1}{2} H_0 \right) + \gamma > 0$, i.e. $\Lambda_{2,3}^2(\lambda, \varepsilon) > 0$, which is a natural assumption, since

$$\tilde{\lambda}_{\text{tip}} = \tilde{\lambda}^+(0) = -\frac{2\gamma}{2\tau - H_0} < 0 \quad (4.16)$$

determines the ‘tip’ of σ_{ess} (recall that $H_0 - 2\tau < 0$), i.e. $t_2(\tilde{\lambda})$ is not defined if $\tilde{\lambda} \leq \tilde{\lambda}_{\text{tip}}$. By definition, $\Delta_{\text{fast}} v_\xi$ is given by (4.8). Since, at leading order $V_h(\xi) = V_h(0) = v_0$ and $U_h(\xi) = u_0(\xi; v_0)$ (uniformly) in I_f (Theorem 2.3), and since $u_0(\xi; v_0)$ decays exponentially fast on the (fast) ξ -scale, it follows that

$$\Delta_{\text{fast}} v_\xi = \varepsilon^2 H_0 \int_{-\infty}^{\infty} \{2 [2u_0^2(\xi; v_0) - 1 - v_0] u_0(\xi; v_0) u_{\text{in}}(\xi; v_0) - u_0^2(\xi; v_0)\} d\xi + \mathcal{O}(\varepsilon^2 \sqrt{\varepsilon}), \quad (4.17)$$

where $u_{\text{in}}(\xi; v_0)$ is the (uniquely determined) bounded solution of the inhomogeneous problem

$$u_{\xi\xi} + (1 + v_0 - 3u_0^2(\xi; v_0))u = -u_0(\xi; v_0).$$

Since we already know one solution of the homogeneous problem, $u(\xi) = u_{0,\xi}(\xi; v_0)$, we can determine $u_{\text{in}}(\xi; v_0)$ explicitly,

$$u_{\text{in}}(\xi; v_0) = \frac{1}{2(1 + v_0)} (u_0(\xi; v_0) + \xi u_{0,\xi}(\xi; v_0)). \quad (4.18)$$

Thus, by (2.3), $\Delta_{\text{fast}} v_\xi$ can be computed explicitly (at leading order),

$$\Delta_{\text{fast}} v_\xi = -\varepsilon^2 H_0 \sqrt{2} \sqrt{1 + v_0} + \mathcal{O}(\varepsilon^2 \sqrt{\varepsilon}).$$

Combining this with (4.15) yields an explicit expression for $t_2(\tilde{\lambda})$,

$$t_2(\tilde{\lambda}, \varepsilon) = 1 - H_0 \sqrt{\frac{2(1 + v_0)}{\tilde{\lambda}(\tau - \frac{1}{2}H_0) + \gamma}} + \mathcal{O}(\sqrt{\varepsilon}) \quad (4.19)$$

for $\tilde{\lambda} > \tilde{\lambda}_{\text{tip}}$ (4.16). It follows that $t_2(\tilde{\lambda}) \geq 1 + \mathcal{O}(\sqrt{\varepsilon})$ for $H_0 \leq 0$ and $t_2(\tilde{\lambda}) < 1 + \mathcal{O}(\sqrt{\varepsilon})$ for $H_0 > 0$. Hence, $t_2(\tilde{\lambda})$ cannot have zeroes if $H_0 \leq 0$. In other words, there cannot be an eigenvalue near the tip of the essential spectrum in case **(ii)** of Theorem 2.3. On the other hand, $t_2(\tilde{\lambda})$ can be 0 for $H_0 > 0$, i.e. in case **(i)** of Theorem 2.3 there indeed is a ‘new’ slow-fast eigenvalue of (3.1), it is given by

$$\lambda_{\text{edge}} = \varepsilon^2 \tilde{\lambda}_{\text{edge}} = \frac{-2\gamma + H_0^2(1 + v_0)}{2\tau - H_0} \varepsilon^2 + \mathcal{O}(\varepsilon^2 \sqrt{\varepsilon}) > \varepsilon^2 \tilde{\lambda}_{\text{tip}} = \lambda_{\text{tip}} \quad (4.20)$$

(4.16). Note that the eigenvalue λ_{edge} merges with λ_{tip} , and thus with σ_{ess} as $H_0 \downarrow 0$. This is of course a leading order result, the accuracy of our analysis only allows us to conclude that $|\lambda_{\text{tip}} - \lambda_{\text{edge}}| \leq \mathcal{O}(\varepsilon^2 \sqrt{\varepsilon})$ as $H_0 \downarrow 0$, and that λ_{edge} does not exist for $H_0 < 0$. Nevertheless, we conclude that λ_{edge} appears from the essential spectrum as H_0 increases through 0. In other words, λ_{edge} is created, or annihilated, by an edge bifurcation. Note that the new eigenvalue appears exactly as σ_{ess} becomes complex valued (section 3.1, Figure 3.1).

The existence, or non-existence of λ_{edge} is crucial to the character of the destabilization (see also the numerical simulations in section 5). For $H_0 < 0$, the front solution $(U_h(\xi), V_h(\xi))$ destabilizes as γ , or equivalently G_1 , crosses through 0. The destabilization is due to the essential spectrum, which implies that also the ‘background states’ $(U(x, t), V(x, t)) \equiv (\pm 1, 0)$ destabilize at $\gamma = 0$. However, in the case $H_0 > 0$ the eigenvalue is λ_{edge} is $\varepsilon^2 H_0^2(1 + v_0)/(2\tau - H_0)$ ahead of σ_{ess} (4.20), in the sense that it reaches the axis $\text{Re}(\lambda) = 0$ before σ_{ess} as $\gamma > 0$ decreases to 0. Thus, if $H_0 > 0$ the front solution $(U_h(\xi), V_h(\xi))$ destabilizes by an element of the discrete spectrum of (3.1) at $\gamma_{\text{double}} = \frac{1}{2}H_0^2(1 + v_0) + \mathcal{O}(\sqrt{\varepsilon}) > 0$. As a consequence, the background states $(\pm 1, 0)$ remain stable as $(\tilde{U}_h(\xi), \tilde{V}_h(\xi))$ destabilizes for $H_0 > 0$, contrary to the case $H_0 < 0$. The bifurcation at γ_{double} is associated to the saddle-node bifurcation of heteroclinic orbits described in Theorem 2.3.

THEOREM 4.6. *Assume that $G(V) = -\varepsilon^2 \gamma$, $H(U^2, V) = H_0 U^2$, $H_0 - 2\tau < 0$ and $\mathcal{O}(1)$, and that $\varepsilon > 0$ is small enough.*

(i) *Let $(U_h^{+,1}(\xi), V_h^{+,1}(\xi))$ and $(U_h^{+,2}(\xi), V_h^{+,2}(\xi))$ be the two types of heteroclinic front solutions that exist for $H_0 > 0$ and $\gamma \geq \gamma_{\text{double}} = \frac{3}{2}H_0^2 + \mathcal{O}(\sqrt{\varepsilon})$ with, at leading order, $0 < V_h^{+,1}(0) = v_1 \leq 2 \leq v_2 = V_h^{+,2}(0)$ (Theorem 2.3). The front solution $(U_h^{+,1}(\xi), V_h^{+,1}(\xi))$ is asymptotically stable for $\gamma > \gamma_{\text{double}}$, the front $(U_h^{+,2}(\xi), V_h^{+,2}(\xi))$ unstable; $(U_h^{+,1}(\xi), V_h^{+,1}(\xi))$ destabilizes by an element of the discrete spectrum, λ_{edge} , at $\gamma = \gamma_{\text{double}}$ and merges with $(U_h^{+,2}(\xi), V_h^{+,2}(\xi))$ in a saddle-node bifurcation of heteroclinic orbits.*

(ii) Let $(U_h^+(\xi), V_h^+(\xi))$ be a heteroclinic front solution that exist for $H_0 < 0$ and (all) $\gamma > 0$ (Theorem 2.3); $(U_h^+(\xi), V_h^+(\xi))$ is asymptotically stable for all $\gamma > 0$, it is destabilized at $\gamma = 0$ by the essential spectrum σ_{ess} .

REMARK 4.7. As in the regular case, spectral stability implies asymptotic nonlinear stability in this super-slow case, since the linear operator associated to the stability problem remains sectorial as long as $\varepsilon > 0$.

Proof of Theorem 4.6. We first note that the condition $H_0 - 2\tau < 0$ and $\mathcal{O}(1)$ determines that σ_{ess} can only cross, or come close to, the $\text{Re}(\lambda) = 0$ -axis at $\lambda = 0$ (Lemma 3.2 with $G_1 = \mathcal{O}(\varepsilon^2)$).

(i) The eigenvalue ‘in front of’ σ_{ess} , $\lambda_{\text{edge}}^{1,2}(v_{1,2})$, is given by (4.20), where $v_0 > 0$ is a solution of $9\gamma v^2 = 2H_0^2(1+v)^3$, and $v_0 = v_1 \leq 2$ (at leading order) for $(U_h^{+,1}(\xi), V_h^{+,1}(\xi))$, while $v_0 = v_2 \geq 2$ (at leading order) for $(U_h^{+,2}(\xi), V_h^{+,2}(\xi))$ – Theorem 2.3. Thus, by (4.20) $-\lambda_{\text{edge}}^1(v_1) < 0$ and $\lambda_{\text{edge}}^2(v_2) > 0$ if $\gamma < \gamma_{\text{double}} = \frac{3}{2}H_0^2 + \mathcal{O}(\sqrt{\varepsilon})$. As a consequence, $\lambda_{\text{edge}}^1(v_1) \uparrow 0$ and $\lambda_{\text{edge}}^2(v_2) \downarrow 0$ as $\gamma \downarrow \gamma_{\text{double}}$, at which the saddle-node bifurcation takes place..

(ii) We have already shown that there can be no eigenvalues in front of the tip of σ_{ess} . Therefore, the statement of the Theorem follows. \square

REMARK 4.8. Since $t_2(\lambda) = 0$, the slow-fast eigenfunction associated to the bifurcation at $\gamma = \gamma_{\text{double}}$ is given by $\phi_2(\xi)$. It follows from Lemmas 3.7 and 3.8 that the u -component of ϕ_2 is odd, and the v -component even, as function of ξ .

4.3. Bifurcations in the general super-slow problem. We now consider the stability of a front solution in the general super-slow limit. Thus, we assume we have established the existence of a front $(U_h(\xi), V_h(\xi))$ for a certain given function $H(U^2, V)$ (Theorem 2.5). To analyze its stability, we again try to determine $t_2(\lambda)$ by measuring $\Delta_{\text{fast}}v_\xi$ and $\Delta_{\text{slow}}v_\xi$.

In order to determine $\Delta_{\text{slow}}v_\xi$ we follow the derivation of (4.13) in the previous section. Hence, we again conclude that non-trivial eigenvalues near 0 are only possible for $\lambda = \mathcal{O}(\varepsilon^2)$, thus we again introduce $\tilde{\lambda}$ (4.12) (see also the proof of Theorem 4.10 for more details on the necessity of this scaling). Note that both G_1 and λ are now $\mathcal{O}(\varepsilon^2)$, thus, we can immediately obtain a leading order expression for $\Delta_{\text{fast}}v_\xi$ in terms of $H(U^2, V)$,

$$\Delta_{\text{fast}}v_\xi = \varepsilon^2 \int_{-\infty}^{\infty} \left\{ 2 \left[H(u_0^2, v_0) - (1 + v_0 - u_0^2) \frac{\partial H}{\partial U^2}(u_0^2, v_0) \right] u_0 u_{\text{in}} - \left[H(u_0^2, v_0) - (1 + v_0 - u_0^2) \frac{\partial H}{\partial V}(u_0^2, v_0) \right] \right\} d\xi + \mathcal{O}(\varepsilon^2 \sqrt{\varepsilon}) \quad (4.21)$$

(3.1), where $u_{\text{in}}(\xi)$ is given in (4.18) – recall that $v = 1 + \mathcal{O}(\sqrt{\varepsilon})$ in I_f . As in the previous section, we have approximated $U_h(\xi)$ by $u_0(\xi; v_0)$ (2.3), $V_h(\xi)$ by v_0 and I_f by \mathbb{R} (Theorem 2.5). Note that the integral converges and that $\Delta_{\text{fast}}v_\xi$ is (at leading order) independent of γ and $\tilde{\lambda}$.

It is in principle possible to determine $\Delta_{\text{slow}}v_\xi$ in terms of $t_2(\lambda)$ from (4.13), however, this equation is in general not of constant coefficients type (unlike for the example problem in section 4.2). If we introduce the super-slow coordinate X by $X = \varepsilon x = \varepsilon^2 \xi$, we can write (4.13) as

$$v_{XX} = \left\{ \tilde{\lambda} \left[\tau - \frac{H(1 + V_h(X), V_h(X))}{2(1 + V_h(X))} \right] + \gamma + \mathcal{O}(\varepsilon^2) \right\} v, \quad (4.22)$$

i.e. the functions $V_h(X)$ introduce explicit X -dependent terms in the equation (section 2.3, $V_h(X)$ behaves as $e^{\mp \sqrt{\gamma} X}$ on $\mathcal{M}_\varepsilon^\pm$). Nevertheless, we can in principle determine the v -components of the solution $\phi_2(\xi)$ of (3.2) outside the fast region I_f . However, the analysis is much less transparent. For instance, the decomposition (4.5) as in Lemma 4.1 now only holds for $X \gg 1$, therefore the relation between $t_3(\tilde{\lambda})$ and $t_2(\tilde{\lambda})$ that is obtained from the value of v in I_f will in general be more complicated than in (4.6). Moreover, $\tilde{\lambda} \left[\tau - \frac{H(1 + V_h(X), V_h(X))}{2(1 + V_h(X))} \right] + \gamma$ might change sign as function of X , so that the solution $v(X)$ of (4.22) can have oscillatory parts.

Thus, we conclude that it is not a straightforward extension of the approach in previous section to determine $t_2(\tilde{\lambda})$ for general values of $\tilde{\lambda}$. It should also be noted that a similar problem occurs in the regular case, in the study of possible eigenvalues near $\lambda^\pm(0)$ (Lemma 4.2). If one introduces

$\tilde{\lambda}^\pm$ by $\lambda = \lambda^\pm(0) + \varepsilon\tilde{\lambda}^\pm$, and derives the leading order equation for v_{xx} (4.3) in this case, then one finds an equation like (4.22), i.e. an equation with spatially dependent coefficients (these x -dependent terms originate from the $\mathcal{O}(\varepsilon)$ corrections corresponding to $V_h(x) = \mathcal{O}(\varepsilon)$ in (4.2) and (4.3)). Hence, at this point it is not yet possible to determine in full detail whether or not eigenvalues exist near the tips of σ_{ess} for general nonlinearities $H(U^2, V)$ and general λ . Moreover, it is also not possible to explicitly describe how and when eigenvalues appear from, or disappear into, σ_{ess} . On the other hand, it is clear from (4.21) and (4.22) that the number of zeros of $t_2(\tilde{\lambda})$ depends (for instance) on H_0 . It thus follows that eigenvalues will be created/annihilated near the tip of σ_{ess} in the general case (like in the example system considered in the previous section). The analysis of eigenvalues near the tip of σ_{ess} is therefore a continuing subject of research (in progress, see also section 5).

Nevertheless, the value $\lambda = \tilde{\lambda} = 0$ is, of course, especially relevant for the stability analysis of the front, and, equation (4.22) is again of constant coefficients type at leading order for this special value of λ . Hence, for $\lambda = 0$ we can obtain the equivalent of Lemma 4.1, so that it follows that

$$\Delta_{\text{slow}} v_\xi|_{\lambda=0} = 2\varepsilon^2(t_2(0) - 1)\sqrt{\gamma} + \mathcal{O}(\varepsilon^2\sqrt{\varepsilon}). \quad (4.23)$$

Note that eventually it becomes clear at this point why the choice $G_1 = -\varepsilon^2\gamma$ is the most relevant scaling of G_1 . With this scaling the ‘jumps’ $\Delta_{\text{slow}}v_\xi$ and $\Delta_{\text{fast}}v_\xi$ (4.21) are of the same magnitude in ε at $\lambda = 0$. Therefore, $t_2(0, \varepsilon)$ is asymptotically close to 1 for all G_1 with $|G_1| \gg \varepsilon^2$ – see Lemma 4.2 and its proof. Thus, the stability problem (3.1) can only have a double eigenvalue at 0 if $G_1 = \mathcal{O}(\varepsilon^2)$. This establishes a significant link between the stability analysis and the existence analysis of section 2, since it is clear from the analysis there that the scaling $G_1 = \mathcal{O}(\varepsilon^2)$ is also the most relevant scaling for the (super-slow) existence problem (Remark 2.2). Moreover, this link is even much more explicit.

THEOREM 4.9. *Assume that $G(V) = -\varepsilon^2\gamma$, that $H_0 - 2\tau < 0$ and $\mathcal{O}(1)$, and that $\varepsilon > 0$ is small enough. Let the front solution $(U_h(\xi; \varepsilon), V_h(\xi; \varepsilon))$ be a heteroclinic solution that corresponds to an intersection $T_\sigma^- \cap W^u(-1, 0, 0, 0)|_{\mathcal{M}_\varepsilon^-}$ as described in Theorem 2.5. The stability problem associated to the front solution has a double eigenvalue at $\lambda = 0$ if and only if the intersection $T_\sigma^- \cap W^u(-1, 0, 0, 0)|_{\mathcal{M}_\varepsilon^-}$ is non-transversal. If the intersection $T_\sigma^- \cap W^u(-1, 0, 0, 0)|_{\mathcal{M}_\varepsilon^-}$ is a second order contact, then the front bifurcates at*

$$0 < \gamma_{\text{double}} = \frac{1}{4(1+v_0)^2} \left[\int_{-\infty}^{\infty} (1 + v_0 - u_0^2)H(u_0^2, v_0)d\xi + 2 \int_{-\infty}^{\infty} (1 + v_0 - u_0^2)[u_0^2 \frac{\partial H}{\partial V^2}(u_0^2, v_0) + (1 + v_0) \frac{\partial H}{\partial V}(u_0^2, v_0)]d\xi \right]^2 \quad (4.24)$$

by merging with another front solution in a saddle-node bifurcation of heteroclinic orbits.

Proof. First, we recall from section 2.3 that a heteroclinic connection that corresponds to the intersection of $W^u(-1, 0, 0, 0)|_{\mathcal{M}_\varepsilon^-} = \{q = \varepsilon\sqrt{\gamma}v\}$ and T_σ^- is determined by (2.15). This is of course a leading order approximation. In the proof of this Theorem we refrain from mentioning this obvious fact at several places. To determine the v_0 -dependence of the right hand side of this relation, we define $w_0(\xi)$ as the (monotonically increasing) heteroclinic solution of $\ddot{w} + (1-w^2)w = 0$. It follows that

$$u_0(\xi; v_0) = \sqrt{1+v_0}w_0(\sqrt{1+v_0}\xi), \quad w_0(t) = \tanh \sqrt{\frac{1}{2}}t \quad (4.25)$$

(2.3). Replacing $u_0(\xi; v_0)$ by $w_0(t)$ in (2.15) yields

$$\sqrt{\gamma}v_0 = \frac{1}{2}\sqrt{1+v_0} \int_{-\infty}^{\infty} (1 - w_0^2)H((1+v_0)w_0^2, v_0)dt. \quad (4.26)$$

Thus, $T_o^- \cap W^u(-1, 0, 0, 0)|_{\mathcal{M}_\varepsilon^-}$ is non-transversal if (2.15) holds and

$$\begin{aligned} \sqrt{\gamma} &= \frac{1}{2} \frac{\partial}{\partial v_0} \left\{ \sqrt{1+v_0} \int_{-\infty}^{\infty} (1-u_0^2) H((1+v_0)w_0^2, v_0) dt \right\} \\ &= \frac{1}{4\sqrt{1+v_0}} \int_{-\infty}^{\infty} (1-u_0^2) H((1+v_0)w_0^2, v_0) dt \\ &\quad + \frac{1}{2} \sqrt{1+v_0} \int_{-\infty}^{\infty} (1-u_0^2) \left[w_0^2 \frac{\partial H}{\partial U^2}((1+v_0)w_0^2, v_0) + \frac{\partial H}{\partial V}((1+v_0)w_0^2, v_0) \right] dt \\ &= \frac{1}{2(1+v_0)} \int_{-\infty}^{\infty} (1+v_0-u_0^2) H(u_0^2, v_0) d\xi \\ &\quad + \frac{1}{1+v_0} \int_{-\infty}^{\infty} (1+v_0-u_0^2) \left[u_0^2 \frac{\partial H}{\partial U^2}(u_0^2, v_0) + (1+v_0) \frac{\partial H}{\partial V}(u_0^2, v_0) \right] d\xi, \end{aligned} \quad (4.27)$$

by re-introducing $u_0(\xi; v_0)$. Note that (4.24) follows from this equation. The expression for $t_2(0, \varepsilon)$ is determined by (4.21), (4.23) and (4.18),

$$t_2(0, \varepsilon) = 1 - \frac{\mathcal{I}_1 + \mathcal{I}_2 + \mathcal{I}_3}{2\sqrt{\gamma}(1+v_0)} + \mathcal{O}(\sqrt{\varepsilon}),$$

where

$$\begin{aligned} \mathcal{I}_1 &= \int_{-\infty}^{\infty} (1+v_0-u_0^2) H(u_0^2, v_0) d\xi, \\ \mathcal{I}_2 &= \int_{-\infty}^{\infty} (1+v_0-u_0^2) \left[u_0^2 \frac{\partial H}{\partial U^2}(u_0^2, v_0) + (1+v_0) \frac{\partial H}{\partial V}(u_0^2, v_0) \right] d\xi, \\ \mathcal{I}_3 &= \int_{-\infty}^{\infty} \left[(1+v_0-u_0^2) \frac{\partial H}{\partial U^2}(u_0^2, v_0) - H(u_0^2, v_0) \right] \xi u_0 u_{0,\xi} d\xi. \end{aligned} \quad (4.28)$$

We find by partial integration that

$$\mathcal{I}_3 = \int_{-\infty}^{\infty} \frac{1}{2} \xi \frac{\partial}{\partial \xi} \left[(1+v_0-u_0^2) H(u_0^2, v_0) \right] d\xi = -\frac{1}{2} \mathcal{I}_1,$$

which implies that

$$t_2(0, \varepsilon) = 1 - \frac{\mathcal{I}_1 + 2\mathcal{I}_2}{4\sqrt{\gamma}(1+v_0)} + \mathcal{O}(\sqrt{\varepsilon}),$$

so that we can conclude by (4.28) that $t_2(0, \varepsilon) = 0$ is equivalent to the non-transversality condition (4.27). Hence, a double eigenvalue of (3.1) coincides with a saddle-node bifurcation of heteroclinic orbits, unless the tangency between T_o^- and $W^u(-1, 0, 0, 0)|_{\mathcal{M}_\varepsilon^-}$ is degenerate. \square

Finally, we can turn to the question about the character of the destabilization of the regular front solution, that has been studied in sections 2.1 and 4.1, as G_1 approaches 0. In order to do so, we first note that the existence problem for the regular case can be recovered from that of the singular limit by re-introducing $G_1 = -\gamma\varepsilon^2$ in the existence condition (2.15). This implies that v_0 must become $\mathcal{O}(\varepsilon)$ and that

$$\sqrt{-G_1}v_0 = \varepsilon \frac{1}{2} \int_{-\infty}^{\infty} (1-u_0^2) H(u_0^2, 0) d\xi + \mathcal{O}(\varepsilon\sqrt{\varepsilon}), \quad (4.29)$$

which is equivalent to (2.4) in Theorem 2.1. Thus, the structure of the front $(U_h(\xi), V_h(\xi))$ as function of $G_1 \uparrow 0$ can be determined by tracing the intersection $T_o^- \cap W^u(-1, 0, 0, 0)|_{\mathcal{M}_\varepsilon^-}$ in the super-slow limit as $W^u(-1, 0, 0, 0)|_{\mathcal{M}_\varepsilon^-} = \{q = \varepsilon\sqrt{\gamma}v\}$ goes down from being almost vertical ($G_1 = \mathcal{O}(1)$, $\gamma = \mathcal{O}(1/\varepsilon^2)$) to horizontal ($G_1 = \gamma = 0$). Note that this process determines a unique ‘regular’ element in the intersection $T_o^- \cap W^u(-1, 0, 0, 0)|_{\mathcal{M}_\varepsilon^-}$, all other elements of $T_o^- \cap W^u(-1, 0, 0, 0)|_{\mathcal{M}_\varepsilon^-}$ do not persist in the regular limit $\gamma = \mathcal{O}(1/\varepsilon^2)$ (here, we do not pay attention to possible heteroclinic connections that have $v_0 \gg 1$ as $\gamma \gg 1$). It depends on the sign of $\frac{1}{2} \int_{-\infty}^{\infty} (1-u_0^2) H(u_0^2, 0) d\xi$ whether v_0 will be positive or negative (4.29), i.e. whether the regular intersection $T_o^- \cap W^u(-1, 0, 0, 0)|_{\mathcal{M}_\varepsilon^-}$ travels through the first or through the third quadrant of the (v, q) -plane as γ decreases. Since $H(U^2, V)$ is smooth, we can make a distinction between two different types of behavior:

Type D The regular element of $T_o^- \cap W^u(-1, 0, 0, 0)|_{\mathcal{M}_\varepsilon^-}$ merges at a certain critical value of $G_1 = -\varepsilon^2\gamma < 0$ with another element of $T_o^- \cap W^u(-1, 0, 0, 0)|_{\mathcal{M}_\varepsilon^-}$ in a saddle-node bifurcation of heteroclinic orbits.

Type E The regular element of $T_o^- \cap W^u(-1, 0, 0, 0)|_{\mathcal{M}_\varepsilon^-}$ exists up to the limit $G_1 = 0$.

Note that T_o^- approaches $(-1, 0)$ as $v_0 \downarrow -1$ (4.26), so that an element of $T_o^- \cap W^u(-1, 0, 0, 0)|_{\mathcal{M}_\varepsilon^-}$ can only reach the singular region $\{v_0 \leq -1\}$ at $\gamma = 0$, which indeed implies that there can only be orbits of type D and E in the third quadrant. We can now describe the destabilization of the regular fronts as G_1 approaches 0.

THEOREM 4.10. *Assume that $G(V) = -\varepsilon^2\gamma$, that $H_0 - 2\tau < 0$ and $\mathcal{O}(1)$, and that $\varepsilon > 0$ is small enough. Consider the heteroclinic front solution $(U_h(\xi), V_h(\xi))$ determined in Theorem 2.1 for $G_1 < 0$ and $\mathcal{O}(1)$ and in Theorem 2.5 for $G_1 = \mathcal{O}(\varepsilon^2)$. If the front is of type D as G_1 becomes $\mathcal{O}(\varepsilon^2)$, then it is asymptotically stable up to $G_1 = -\varepsilon^2\gamma_{\text{double}} < 0$ (4.24) and it is destabilized by a (discrete) eigenvalue through a saddle-node bifurcation of heteroclinic orbits. A front solution of type E is stable up to $G_1 = 0$ and it is destabilized by the essential spectrum.*

Thus, the destabilization of a regular front solution in the limit $G_1 \uparrow 0$ is completely determined by the geometrical structure of $T_o^- \cap W^u(-1, 0, 0, 0)|_{\mathcal{M}_\varepsilon^-}$ in the super-slow limit. Note that Figure 2.3 presents examples of type D and type E behavior.

Proof. The proof of this Theorem is a bit more subtle than a priori might be expected, since in general we do not have control over the eigenvalues of (3.1) near the tip of σ_{ess} (see also Remark 4.11), except that these eigenvalues must be $\mathcal{O}(\varepsilon^2)$ close to σ_{ess} (see also below). Thus, for instance the following scenario for a type D orbit might be possible as γ decreases to γ_{double} : two eigenvalues bifurcate (subsequently) from σ_{ess} (as real eigenvalues), merge and become a pair of complex eigenvalues. This pair crosses through the $\text{Re}(\lambda) = 0$ axis at $\gamma_{\text{Hopf}} > \gamma_{\text{double}}$, and touch down again on the real axis. At γ_{double} one of these eigenvalues returns to $\text{Re}(\lambda) = 0$. Thus, in this scenario, there already exists an unstable eigenvalue at $\gamma = \gamma_{\text{double}}$; moreover, the front destabilizes by a Hopf bifurcation at $\gamma_{\text{Hopf}} > \gamma_{\text{double}}$.

Let us first note that a destabilization by a Hopf bifurcation is the only alternative to the statements of the Theorem, since eigenvalues either move through 0, or (in pairs) through the $\text{Re}(\lambda) = 0$ axis. If we can show that a Hopf bifurcation cannot occur for $\gamma > \gamma_{\text{double}}$, then it is clear that for type D orbits $\lambda_{\text{edge}} < 0$ for $\gamma > \gamma_{\text{double}}$ and that there is no unstable spectrum at $\gamma = \gamma_{\text{double}}$ (this follows from Theorem 4.3: if γ is $\gg \mathcal{O}(1/\varepsilon)$, all non-trivial eigenvalues must be in $\{\text{Re}(\lambda) < -\varepsilon\}$, hence, by decreasing γ , there is one eigenvalue, λ_{edge} , that is the first to reach 0; this happens at the saddle-node bifurcation (Theorem 4.9), i.e. at $\gamma = \gamma_{\text{double}}$). Thus, the front is stable for $\gamma > \gamma_{\text{double}}$. The same argument can be used to establish the non-existence of unstable spectrum for type E orbits, if there are no Hopf bifurcations possible.

To show that there cannot be Hopf bifurcations (for $H_0 - 2\tau < 0$ and $\mathcal{O}(1)$, see section 5), we first ascertain that λ must be $\mathcal{O}(\varepsilon^2)$, i.e. that (4.12) is the correct scaling. This follows by the same arguments as in the proof of Lemma 4.2. If $\Delta_{\text{slow}}v_\xi \gg \Delta_{\text{fast}}v_\xi$, then there cannot be an eigenvalue. Thus, it follows from (4.11) that $|\lambda|$ must indeed be $\mathcal{O}(\varepsilon^2)$ near $\lambda^+(0)$. Hence, even if there is a Hopf bifurcation, it will be $\mathcal{O}(\varepsilon^2)$ close to 0. Next, we realize that this situation is covered by (4.17) for the jump through the fast field, thus, $\Delta_{\text{fast}}v_\xi$ is real (at leading order), independent of $\tilde{\lambda}$. However, it follows from (4.22) that $\Delta_{\text{slow}}v_\xi$ cannot be real if $\tilde{\lambda}$ is complex-valued. Hence, there cannot be a Hopf bifurcation $\mathcal{O}(\varepsilon^2)$ close to $\lambda = 0$. \square

REMARK 4.11. By the same geometrical arguments (that are based on Theorem 4.9) we can describe the character of the bifurcations as function γ in the stability problem associated to a heteroclinic orbit that corresponds to a non-regular element of $T_o^- \cap W^u(-1, 0, 0, 0)|_{\mathcal{M}_\varepsilon^-}$. However, it should be noted that, in general, we do not have enough information on the spectrum of (3.1) to establish the stability of such a front, since we did not determine all possible eigenvalues. In general, we cannot exclude the possibility that various eigenvalues have bifurcated from the essential spectrum for these fronts (in fact, the possible oscillatory character of a solution $v(X)$ of (4.22) strongly suggests that this can happen). Nevertheless, we may for instance conclude that if the regular orbit is of type D, then it merges with a non-regular orbit at γ_{double} that is unstable

for any $\gamma > \gamma_{\text{double}}$ for which it exists.

REMARK 4.12. The most simple example one can consider is $H(U^2, V) \equiv H_0$. This corresponds to the case in which the function $F(U^2, V)$ in (1.1) is (the most general) linear function of U^2 and V with parameters G_1 and H_0 (i.e. $F(U^2, V) = H_0 + (H_0 + G_1)V - H_0U^2$, recall that $F(1, 0)$ must be 0). In this case, T_o^- is given by $\{q = 2\varepsilon H_0 \sqrt{1 + v_0} + \mathcal{O}(\varepsilon^2)\}$, so that $W^u(-1, 0, 0, 0)|_{\mathcal{M}_\varepsilon^-}$ can never be tangent to T_o^- . Hence in this case, there is a uniquely determined front solution of type E for any $H_0 \neq 0$ and $G_1 < 0$, i.e. the front solution is stable up to $G_1 = 0$ and it is destabilized by the essential spectrum.

REMARK 4.13. We did not consider the degenerate case in which $H(U^2, V)$ is such that $H(1 + V, V) \equiv 0$ (section 1), i.e. functions H such that $H(U^2, V) = (1 + V - U^2)\tilde{H}(U^2, V)$ for some smooth function \tilde{H} . In a sense, this is a much more simple problem, for instance since in the super-slow limit, the stability problem in the slow field is automatically of constant coefficients type (at leading order), see (4.11), (4.22). Moreover, it is also clear from these same relations that we can find $\mathcal{O}(1)$ instead of $\mathcal{O}(\varepsilon^2)$ eigenvalues in this case if $\tau = \mathcal{O}(\varepsilon^2)$. In fact, the situation is very much like the stability analysis of (homoclinic) pulses in mono-stable systems in [4, 5]. For instance, as in [4, 5], potential eigenvalues are no longer ‘slaved’ to the tips of the essential spectrum or to the eigenvalues of the fast reduced limit (Lemma 4.2). Moreover, the ‘natural’ persistence result of Lemma 4.4 is also not valid in this case, in general.

5. Simulations and Discussion.

5.1. Simulations. We now examine numerically the difference between the two types of bifurcations discussed in Theorems 4.6 and 4.10. We consider the example system of sections 2.2 and 4.2 for $H_0 > 0$ (case (i), type D) and $H_0 < 0$ (case (ii0), type E). First, we note that in both cases the simulations confirm that the fronts are asymptotically stable up to the analytically determined bifurcation values. In case (i) the front destabilizes at $\gamma < \gamma_{\text{double}}$ due to an eigenvalue in the discrete spectrum. The eigenfunction associated to this type of destabilization is localized to a neighborhood of the front as can be seen in figure 5.1. In this case the front becomes unstable and blows up in finite time, while the background states remain stable. In case (ii), the tip of the essential spectrum becomes positive and the background states become unstable as γ passes through 0. As can be seen in figure 5.1, this destabilization causes the front to collapse. The U component then tends to 0 on the entire real line and the V component grows according to $V_t = V_{xx} + \varepsilon^2|\gamma|V$. Thus, we may conclude that type D or type E orbits indeed exhibit significantly different behavior at the destabilization. These simulations were performed using SPMDf [2], with Neumann boundary conditions at $x = \pm 50$. The initial conditions used in figure (5.1) are given by $U(x, 0) = u_0(x, \varepsilon; v_1)$ (2.3 and $V(x, 0) = v_1 e^{-\varepsilon\sqrt{|\gamma||x|}}$ (as described in Theorem 2.3).

5.2. Hopf bifurcations. As we have seen in section 4.1, in general there can be (complex) eigenvalues near the endpoints $\lambda^\pm(0)$ of σ_{ess} . Thus, if we keep $G_1 < 0$ fixed at an $\mathcal{O}(1)$ value and increase H_0 such that $H_0 + G_1 - 2\tau$ approaches 0, we encounter a similar issue as was studied in the previous section: will the front be destabilized by σ_{ess} at $H_0 = 2\tau - G_1$ or (just) before that, by an eigenvalue? In this case, the bifurcation is of Hopf type, and it is not associated to the existence problem. This problem can in principle be analyzed by the methods developed here, i.e. by determining $t_2(\lambda, \varepsilon)$ through $\Delta_{\text{slow}}v_\xi$ and $\Delta_{\text{fast}}v_\xi$. We have already mentioned the new features of the measuring the slow ‘jump’ $\Delta_{\text{slow}}v_\xi$ in section 4.3. Moreover, since the bifurcation does not occur near $\lambda = 0$, we do not have an explicit formula for $u_{\text{in}}(\xi)$, like (4.18), and it is thus not immediately clear whether it is possible to determine $\Delta_{\text{fast}}v_\xi$. Note that this latter issue is solvable with the hypergeometric functions method developed in [3, 5]. Nevertheless, we do not go deeper into this subject here.

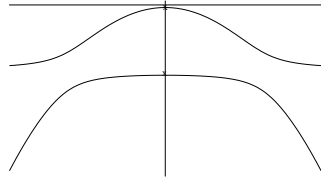
5.3. Planar fronts and stripes. A next step in the study of (planar) stripes, as mentioned in the Introduction, is the stability analysis of planar fronts, i.e. the analysis of the stability of the fronts $(U_h(\xi), V_h(\xi))$ with respect to two-dimensional perturbations (thus, $(U_h(\xi), V_h(\xi))$ represents a planar front that has a trivial structure in the y -direction). The methods developed

here can be used to study this problem (as is also suggested by [7] in which a similar problem has been studied in a mono-stable Gierer-Meinhardt context). It should be noted here that there are several papers in the literature that consider the question of the (non-)persistence of the stability of one-dimensional fronts as two-dimensional planar fronts (see for instance [16, 19, 12, 15]). The analysis in [19, 15] of a class of singularly perturbed bi-stable systems shows that the planar fronts considered there cannot be stable, while it is shown that planar fronts can be stable in a more regular context in [12]. Thus, this is a nontrivial issue. Preliminary analysis of the front solutions considered in this paper indicates that these solutions remain stable as planar fronts in the regular case (i.e. as long as $G_1 < 0$ and $\mathcal{O}(1)$). The analysis of the planar fronts, and their spatially periodic counterparts, the stripe patterns, is the subject of work in progress.

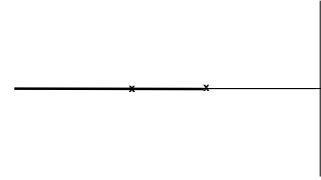
Acknowledgements. D.I. would like to thank NSERC for their support by way of a post doctoral fellowship. A.D. and D.I acknowledge support of the ‘Research Training Network (RTN): Fronts-Singularities’ (RTN contract: HPRN-CT-2002-00274).

REFERENCES

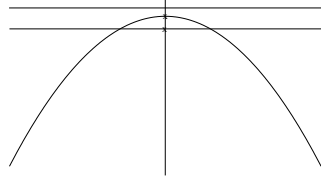
- [1] J. Alexander, R.A. Gardner, C.K.R.T. Jones [1990], A topological invariant arising in the stability analysis of travelling waves, *J. Reine Angew. Math.* **410**, 167–212.
- [2] J.G. Blom, P.A. Zegeling [1994], Algorithm 731: A Moving-Grid Interface for Systems of One-Dimensional Time-Dependent Partial Differential Equations, *ACM Transactions in Mathematical Software*, **20**, 194–214.
- [3] A. Doelman, R. A. Gardner and T.J. Kaper [1998], Stability analysis of singular patterns in the 1-D Gray–Scott model: A matched asymptotics approach, *Physica D* **122**, 1–36.
- [4] A. Doelman, R. A. Gardner, and T.J. Kaper [2002], A stability index analysis of 1-D patterns of the Gray–Scott model, *Memoirs of the AMS* **155** (737).
- [5] A. Doelman, R. A. Gardner, and T.J. Kaper [2001], Large stable pulse solutions in reaction-diffusion equations, *Ind. Univ. Math. J.*, **50**(1), 443–507.
- [6] A. Doelman, T.J. Kaper, and P. Zegeling [1997], Pattern formation in the one-dimensional Gray-Scott model, *Nonlinearity* **10**, 523–563.
- [7] A. Doelman and H. van der Ploeg [2001], Homoclinic stripe patterns, *SIAM J. Appl. Dyn. Syst.* **1**, 65–104.
- [8] D. Henry [1981], ‘*Geometric Theory of Semilinear Parabolic Equations*’, Lecture Notes in Math. **840**, Springer-Verlag.
- [9] N. Fenichel [1979], Geometrical singular perturbation theory for ordinary differential equations, *J. Diff. Eq.* **31**, 53–98.
- [10] R.A. Gardner and C.K.R.T. Jones [1991], Stability of the travelling wave solutions of diffusive predator-prey systems, *Trans. AMS* **327**, 465–524.
- [11] C.K.R.T. Jones [1995], Geometric singular perturbation theory, in *Dynamical systems, Montecatini Terme, 1994*, Lecture Notes in Mathematics **1609**, R. Johnson (ed.), Springer-Verlag.
- [12] T. Kapitula [1997], Multidimensional stability of planar travelling waves, *Trans. Amer. Math. Soc.* **349**, 257–269.
- [13] T. Kapitula [1998], The Evans function and generalized Melnikov integrals, *SIAM J. Math. Anal.* **30**, 273–297.
- [14] T. Kapitula and B. Sandstede [2002], Edge bifurcations for near integrable systems via Evans function techniques, *SIAM J. Math. Anal.* **33**, 1117–1143.
- [15] Y. Nishiura and H. Suzuki [1998], Nonexistence of higher dimensional stable Turing patterns in the singular limit, *SIAM J. Math. Anal.* **29**, 1087–1105.
- [16] T. Ohta, M. Mimura and R. Kobayashi [1989], Higher-dimensional localized patterns in excitable media, *Physica D* **34**, 115–144.
- [17] R.L. Pego, M.I. Weinstein [1992], Eigenvalues, and instabilities of solitary waves, *Philos. Trans. Roy. Soc. London Ser. A* **340**, 47–94.
- [18] C. Robinson [1983], Sustained resonance for a nonlinear system with slowly-varying coefficients, *SIAM J. Math. Anal.* **14**, 847–860.
- [19] M. Taniguchi and Y. Nishiura [1994], Instability of planar interfaces in reaction-diffusion systems, *SIAM J. Math. Anal.* **25**, 99–134.
- [20] E.C. Titchmarsh [1962], *Eigenfunction Expansions Associated with Second-order Differential Equations* (2nd ed.), Oxford Univ. Press.



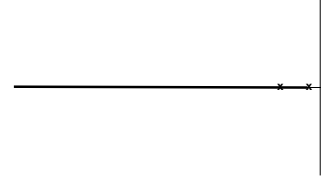
(a) $\text{Re}(\lambda)$ vs k with $H_0 < 0$.



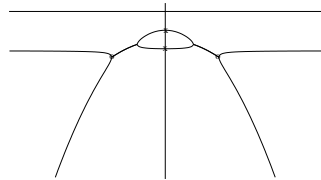
(b) $\text{Re}(\lambda)$ vs $\text{Im}(\lambda)$ with $H_0 < 0$.



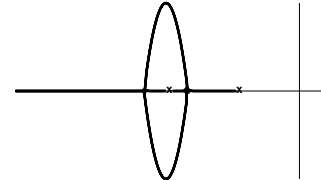
(c) $H_0 = 0$.



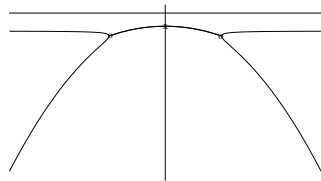
(d) $H_0 = 0$.



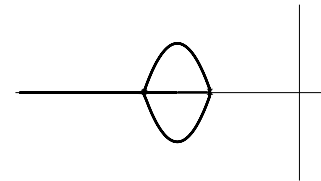
(e) $H_0 \in (0, (\sqrt{2\tau} - \sqrt{-G_1})^2)$.



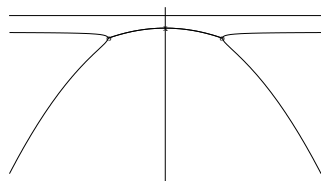
(f) $H_0 \in (0, (\sqrt{2\tau} - \sqrt{-G_1})^2)$.



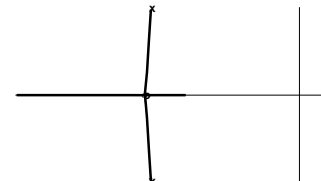
(g) $H_0 = (\sqrt{2\tau} - \sqrt{-G_1})^2$.



(h) $H_0 = (\sqrt{2\tau} - \sqrt{-G_1})^2$.



(i) $H_0 \in ((\sqrt{2\tau} - \sqrt{-G_1})^2, 2\tau - G_1)$.



(j) $H_0 \in ((\sqrt{2\tau} - \sqrt{-G_1})^2, 2\tau - G_1)$.

FIG. 3.1. The five possible different structures of the stable essential spectrum. On the left we plot $\text{Re}(\lambda)$ vs k and on the right $\text{Re}(\lambda)$ vs $\text{Im}(\lambda)$.

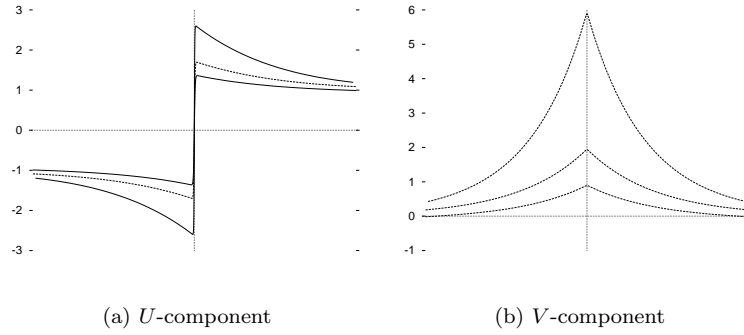


FIG. 5.1. Numerical simulation of destabilization caused by the discrete spectrum, both components blow up in finite time ($H_0 = -1$, $\gamma = 1.4$, $\tau = 1$ and $\varepsilon = 0.1$).

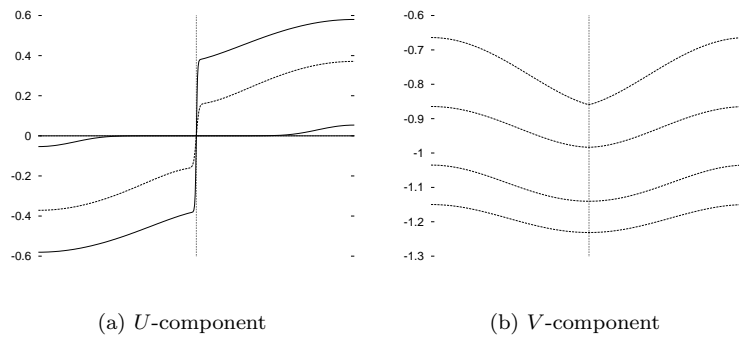


FIG. 5.2. Numerical simulation of destabilization caused by the essential spectrum, $U \rightarrow 0$ and $|V|$ grows slowly and exponentially ($H_0 = 1$, $\gamma = -0.1$, $\tau = 1$ and $\varepsilon = 0.1$).

USING SIAM'S L^AT_EX MACROS*

PAUL DUGGAN†

Abstract. Documentation is given for use of the SIAM L^AT_EX macros. These macros are now compatible with L^AT_EX2_ε. Instructions and suggestions for compliance with SIAM style standards are also included. Familiarity with standard L^AT_EX commands is assumed.

Key words.

AMS subject classifications.

1. Introduction. This file is documentation for the SIAM L^AT_EX macros, and provides instruction for submission of your files.

To accommodate authors who electronically typeset their manuscripts, SIAM supports the use of L^AT_EX. To ensure quality typesetting according to SIAM style standards, SIAM provides a L^AT_EX macro style file. Using L^AT_EX to format a manuscript should simplify the editorial process and lessen the author's proofreading burden. However, it is still necessary to proofread the galley proofs with care.

Electronic files should not be submitted until the paper has been accepted, and then not until requested to do so by someone in the SIAM office. Once an article is slated for an issue, someone from the SIAM office will contact the author about any or all of the following: editorial and stylistic queries, supplying the source files (and any supplementary macros) for the properly formatted article, and handling figures.

When submitting electronic files (electronic submissions) (to tex@siam.org) include the journal, issue, and author's name in the subject line of the message. Authors are responsible for ensuring that the paper generated from the source files exactly matches the paper that was accepted for publication by the review editor. If it does not, information on how it differs should be indicated in the transmission of the file. When submitting a file, please be sure to include any additional macros (other than those provided by SIAM) that will be needed to run the paper.

SIAM uses MS-DOS-based computers for L^AT_EX processing. Therefore all file-names should be restricted to eight characters or less, plus a three character extension.

Once the files are corrected here at SIAM, we will mail the revised proofs to be read against the original edited hardcopy manuscript. We are not set up to shuttle back and forth varying electronic versions of each paper, so we must rely on hard copy of the galleys. The author's proofreading is an important but easily overlooked step. Even if SIAM were not to introduce a single editorial change into your manuscript, there would still be a need to check, because electronic transmission can introduce errors.

The distribution contains the following items: `siamltx.cls`, the main macro package based on `article.cls`; `siam10.clo`, for the ten-point size option; `subeqn.clo`, a style option for equation numbering (see §3 for an explanation); and `siam.bst`, the style file for use with BIB_TE_X. Also included are this file `docultex.tex` and a sample file `lexample.tex`. The sample file represents a standard application of the macros. The rest of this paper will highlight some keys to effective macro use,

*This work was supported by the Society for Industrial and Applied Mathematics

†Society for Industrial and Applied Mathematics, Philadelphia, Pennsylvania. (duggan@siam.org). Questions, comments, or corrections to this document may be directed to that email address.

as well as point out options and special cases, and describe SIAM style standards to which authors should conform.

2. Headings. The top matter of a journal paper falls into a standard format. It begins of course with the `\documentclass` command

```
\documentclass{siamltex}
```

Other class options can be included in the bracketed argument of the command, separated by commas.

Optional arguments include:

final Without this option, lines which extend past the margin will have black boxes next to them to help authors identify lines that they need to fix, by re-writing or inserting breaks. **final** turns these boxes off, so that very small margin breaks which are not noticeable will not cause boxes to be generated.

oneeqnum Normally `siamltex.cls` numbers equations, tables, figures, and theorem environments with a decimal number, composed of the section of the paper, a period, and the number of the enumerated object (example: 1.2). The sequence of numbering is also restarted with each new section, so that, for example, the last equation of section 3 may be 3.10, but the first equation of section 4 would be 4.1. Using **oneeqnum** numbers all equations consecutively throughout a paper with a single digit.

onethmnum Using **onethmnum** numbers all theorem-like environments consecutively throughout a paper with a single digit.

onefignum Using **onethmnum** numbers all figures consecutively throughout a paper with a single digit.

onetabnum Using **onethmnum** numbers all tables consecutively throughout a paper with a single digit.

The title and author parts are formatted using the `\title` and `\author` commands as described in Lamport [3]. The `\date` command is not used. `\maketitle` produces the actual output of the commands.

The addresses and support acknowledgments are put into the `\author` commands via `\thanks`. If support is overall for the authors, the support acknowledgment should be put in a `\thanks` command in the `\title`. Specific support should go following the addresses of the individual authors in the same `\thanks` command.

Sometimes authors have support or addresses in common which necessitates having multiple `\thanks` commands for each author. Unfortunately \LaTeX does not normally allow this, so a special procedure must be used. An example of this procedure follows. Grant information can also be run into both authors' footnotes.

```
\title{TITLE OF PAPER}
```

```
\author{A.~U. Thorone\footnotemark[2]\ \footnotemark[5]
\and A.~U. Thortwo\footnotemark[3]\ \footnotemark[5]
\and A.~U. Thorthree\footnotemark[4]}
```

```
\begin{document}
\maketitle
```

```
\renewcommand{\thefootnote}{\fnsymbol{footnote}}
```

```

\footnotetext[2]{Address of A.~U. Thorone}
\footnotetext[3]{Address of A.~U. Thortwo}
\footnotetext[4]{Address of A.~U. Thorthree}
\footnotetext[5]{Support in common for the first and second
authors.}

\renewcommand{\thefootnote}{\arabic{footnote}}

```

Notice that the footnote marks begin with [2] because the first mark (the asterisk) will be used in the title for date-received information by SIAM, even if not already used for support data. This is just one example; other situations follow a similar pattern.

Following the author and title is the abstract, key words listing, and AMS subject classification number(s), designated using the `{abstract}`, `{keywords}`, and `{AMS}` environments. If there is only one AMS number, the commands `\begin{AM}` and `\end{AM}` are used instead of `{AMS}`. This causes the heading to be in the singular. Authors are responsible for providing AMS numbers. They can be found in the Annual Index of Math Reviews, or through e-Math (telnet e-math.ams.com; login and password are both e-math).

Left and right running heads should be provided in the following way.

```

\pagestyle{myheadings}
\thispagestyle{plain}
\markboth{A.~U. THORONE AND A.~U. THORTWO}{SHORTER PAPER
TITLE}

```

3. Equations and mathematics. One advantage of L^AT_EX is that it can automatically number equations and refer to these equation numbers in text. While plain T_EX's method of equation numbering (explicit numbering using `\leqno`) works in the SIAM macro, it is not preferred except in certain cases. SIAM style guidelines call for aligned equations in many circumstances, and L^AT_EX's `{eqnarray}` environment is not compatible with `\leqno` and L^AT_EX is not compatible with the plain T_EX command `\eqalign` and `\leqalignno`. Since SIAM may have to alter or realign certain groups of equations, it is necessary to use the L^AT_EX system of automatic numbering.

Sometimes it is desirable to designate subequations of a larger equation number. The subequations are designated with (roman font) letters appended after the number. SIAM has supplemented its macros with the `subeqn.clo` option which defines the environment `{subequations}`.

```

\begin{subequations}\label{EKx}
\begin{equation}
y_k = B y_{k-1} + f, \quad k=1,2,3,\ldots
\end{equation}
for any initial vector $ y_0$. Then
\begin{equation}
y_k \rightarrow u \quad \text{\mbox{\quad iff\quad}} \quad \rho(B) < 1.
\end{equation}
\end{subequations}

```

All equations within the `{subequations}` environment will keep the same overall number, but the letter designation will increase.

Clear equation formatting using \TeX can be challenging. Aside from the regular \TeX documentation, authors will find Nicholas J. Higham’s book *Handbook of Writing for the Mathematical Sciences* [2] useful for guidelines and tips on formatting with \TeX . The book covers many other topics related to article writing as well.

Authors commonly make mistakes by using `<`, `>`, `\mid`, and `\parallel` as delimiters, instead of `\langle`, `\rangle`, `|`, and `\|`. The incorrect symbols have particular meanings distinct from the correct ones and should not be confused.

TABLE 3.1
Illustration of incorrect delimiter use.

Wrong		Right	
<code><x, y></code>	<code>< x, y ></code>	<code>\langle x, y\rangle</code>	<code>\langle x, y\rangle</code>
<code>5 < \mid A \mid</code>	<code>5 < A </code>	<code>5 < A </code>	<code>5 < A </code>
<code>6x = \parallel x</code>			
<code>- 1\parallel_{i}</code>	<code>6x = \ x - 1 \ _i</code>	<code>6x = \ x - 1\ _i</code>	<code>6x = \ x - 1\ _i</code>

Another common author error is to put large (and even medium sized) matrices in-line with the text, rather than displaying them. This creates unattractive line spacing problems, and should be assiduously avoided. Text-sized matrices (like $\begin{pmatrix} a & b \\ b & c \end{pmatrix}$) might be used but anything much more complex than the example cited will not be easy to read and should be displayed.

More information on the formatting of equations and aligned equations is found in Lamport [3]. Authors bear primary responsibility for formatting their equations within margins and in an aesthetically pleasing and informative manner.

The SIAM macros include additional roman math words, or “log-like” functions, to those provided in standard \TeX . The following commands are added: `\const`, `\diag`, `\grad`, `\Range`, `\rank`, and `\supp`. These commands produce the same word as the command name in math mode, in upright type.

4. Special fonts. SIAM supports the use of the AMS- \TeX fonts (version 2.0 and later). The package `amsfonts` can be included with the command `\usepackage{amsfonts}`. This package is part of the AMS- \LaTeX distribution, available from the AMS or from the Comprehensive TeX Archive Network (anonymous ftp to ftp.shsu.edu). The blackboard bold font in this font package can be used for designating number sets. This is preferable to other methods of combining letters (such as \mathbb{I} and \mathbb{R} for the real numbers) to produce pseudo-bold letters but this is tolerable as well. Typographically speaking, number sets may simply be designated using regular bold letters; the blackboard bold typeface was designed to fulfil a desire to simulate the limitations of a chalk board in printed type.

4.1. Punctuation. All standard punctuation and all numerals should be set in roman type (upright) even within italic text. The only exceptions are periods and commas. They may be set to match the surrounding text.

References to sections should use the symbol \S , generated by `\S`. (If the reference begins a sentence, the term “Section” should be spelled out in full.) Authors should not redefine `\S`, say, to be a calligraphic \mathcal{S} , because `\S` must be reserved for use as the section symbol.

Authors sometimes confuse the use of various types of dashes. Hyphens (–, -) are used for some compound words (many such words should have no hyphen but must be run together, like “nonzero,” or split apart, like “well defined”). Minus signs (\$-\$, −) should be used in math to represent subtraction or negative numbers. En dashes (–, –) are used for ranges (like 3–5, June–August), or for joined names (like Runge–Kutta). Em dashes (—, —) are used to set off a clause—such as this one—from the rest of the sentence.

4.2. Text formatting. SIAM style preferences do not make regular use of the `{enumerate}` and `{itemize}` environments. Instead, `siamltex.cls` includes definitions of two alternate list environments, `{renumerate}` and `{romannum}`. Unlike the standard itemized lists, these environments do not indent the secondary lines of text. The labels, whether defaults or the optional user-defined, are always aligned flush right.

The `{renumerate}` environment consecutively numbers each item with an arabic numeral followed by a period. This number is always upright, even in slanted environments. (For those wondering at the unusual naming of this environment, it comes from Seroul and Levy’s [4] definition of a similar macro for plain T_EX: `\meti` which is `\item` spelled backwards. Thus `{renumerate}` a portion of `{enumerate}` spelled backwards.)

The `{romannum}` environment consecutively numbers each item with a lower-case roman numeral enclosed in parentheses. This number will always be upright within slanted environments (as in theorems).

5. Theorems and Lemmas. Theorems, lemmas, corollaries, definitions, and propositions are covered in the SIAM macros by the theorem-environments `{theorem}`, `{lemma}`, `{corollary}`, `{definition}` and `{proposition}`. These are all numbered in the same sequence and produce labels in small caps with an italic body. Other environments may be specified by the `\newtheorem` command. SIAM’s style is for Remarks and Examples to appear with italic labels and an upright roman body.

```
\begin{theorem}
Sample theorem included for illustration.
Numbers and parentheses, like equation $(3.2)$, should be set
in roman type. Note that words (as opposed to ‘‘log-like’’
functions) in displayed equations, such as
$$ x^2 = Y^2 \sin z^2 \mbox{ for all } x $$
will appear in italic type in a theorem, though normally
they should appear in roman.\end{theorem}
```

This sample produces Theorem 4.1 below.

THEOREM 5.1. *Sample theorem included for illustration. Numbers and parentheses, like equation (3.2), should be set in roman type. Note that words (as opposed to “log-like” functions) in displayed equations, such as*

$$x^2 = Y^2 \sin z^2 \text{ for all } x$$

will appear in italic type in a theorem, though normally they should appear in roman.

Proofs are handled with the `\begin{proof}` `\end{proof}` environment. A “QED” box □ is created automatically by `\end{proof}`, but this should be preceded with a `\qquad`.

Named proofs, if used, must be done independently by the authors. SIAM style specifies that proofs which end with displayed equations should have the QED box two ems (`\qqquad`) from the end of the equation on line with it horizontally. Below is an example of how this can be done:

```
{\em Proof}. Proof of the previous theorem
```

```
      .
      .
      .
```

```
thus,
```

```
$$
```

```
a^2 + b^2 = c^2 \qqquad\endproof
```

```
$$
```

6. Figures and tables. Figures and tables sometimes require special consideration. Tables in SIAM style are need to be set in eight point size by using the `\footnotesize` command inside the `\begin{table}` environment. Also, they should be designed so that they do not extend beyond the text margins.

SIAM style requires that no figures or tables appear in the references section of the paper. \LaTeX is notorious for making figure placement difficult, so it is important to pay particular attention to figure placement near the references in the text. All figures and tables should be referred to in the text.

SIAM supports the use of `epsfig` for including POSTSCRIPT figures. All POSTSCRIPT figures should be sent in separate files. See the `epsfig` documentation (available via anonymous ftp from CTAN: ftp.shsu.edu) for more details on the use of this style option. It is a good idea to submit high-quality hardcopy of all POSTSCRIPT figures just in case there is difficulty in the reproduction of the figure. Figures produced by other non- \TeX methods should be included as high-quality hardcopy when the manuscript is submitted.

POSTSCRIPT figures that are sent should be generated with sufficient line thickness. Some past figures authors have sent had their line widths become very faint when SIAM set the papers using a high-quality 1200dpi printer.

Hardcopy for non-POSTSCRIPT figures should be included in the submission of the hardcopy of the manuscript. Space should be left in the `{figure}` command for the hardcopy to be inserted in production.

7. Bibliography and Bib \TeX . If using Bib \TeX , authors need not submit the `.bib` file for their papers. Merely submit the completed `.bbl` file, having used `siam.bst` as their bibliographic style file. `siam.bst` only works with Bib \TeX version 99i and later. The use of Bib \TeX and the preparation of a `.bib` file is described in greater detail in [3].

If not using Bib \TeX , SIAM bibliographic references follow the format of the following examples:

```
\bibitem{Ri} {\sc W. Riter},
{\em Title of a paper appearing in a book}, in The Book
Title, E.~D. One, E.~D. Two, and A.~N. Othereditor, eds.,
Publisher, Location, 1992, pp.~000--000.
```

```
\bibitem{AuTh1} {\sc A.~U. Thorone}, {\em Title of paper
```

with lower case letters}, SIAM J. Abbrev. Correctly, 2 (1992), pp.~000--000.

```
\bibitem{A1A2} {\sc A.~U. Thorone and A.~U. Thortwo}, {\em
Title of paper appearing in book}, in Book Title: With All
Initial Caps, Publisher, Location, 1992.
```

```
\bibitem{A1A22} \sameauthor, % generates the 3 em rule
{\em Title of Book{\rm :} Note Initial Caps and {\rm ROMAN
TYPE} for Punctuation and Acronyms}, Publisher,
Location, pp.~000--000, 1992.
```

```
\bibitem{AuTh3} {\sc A.~U. Thorthree}, {\em Title of paper
that's not published yet}, SIAM. J. Abbrev. Correctly, to appear.
```

Other types of references fall into the same general pattern. See the sample file or any SIAM journal for other examples. Authors must correctly format their bibliography to be considered as having used the macros correctly. An incorrectly formatted bibliography is not only time-consuming for SIAM to process but it is possible that errors may be introduced into it by keyboarders/copy editors.

As an alternative to the above style of reference, an alphanumeric code may be used in place of the number (e.g., [A^UTh90]). The same commands are used, but `\bibitem` takes an optional argument containing the desired alphanumeric code.

Another alternative is no number, simply the authors' names and the year of publication following in parentheses. The rest of the format is identical. The macros do not support this alternative directly, but modifications to the macro definition are possible if this reference style is preferred.

8. Conclusion. Many other style suggestions and tips could be given to help authors but are beyond the scope of this document. Simple mistakes can be avoided by increasing your familiarity with how L^AT_EX functions. The books referred to throughout this document are also useful to the author who wants clear, beautiful typography with minimal mistakes.

Appendix. The use of appendices. The `\appendix` command may be used before the final sections of a paper to designate them as appendices. Once `\appendix` is called, all subsequent sections will appear as

Appendix A. Title of appendix. Each one will be sequentially lettered instead of numbered. Theorem-like environments, subsections, and equations will also have the section number changed to a letter.

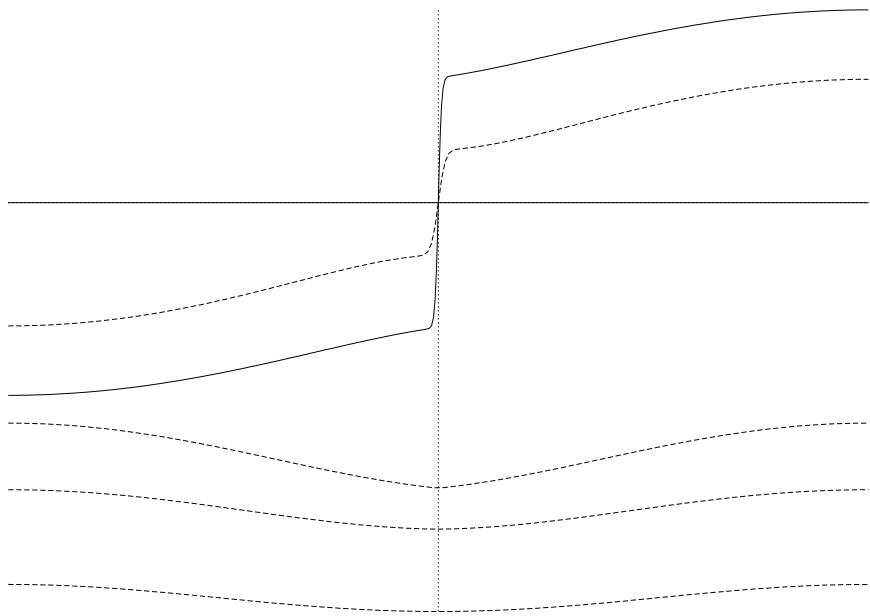
If there is only *one* appendix, however, the `\Appendix` (with a capital letter) should be used instead. This produces only the word **Appendix** in the section title, and does not add a letter. Equation numbers, theorem numbers and subsections of the appendix will have the letter "A" designating the section number.

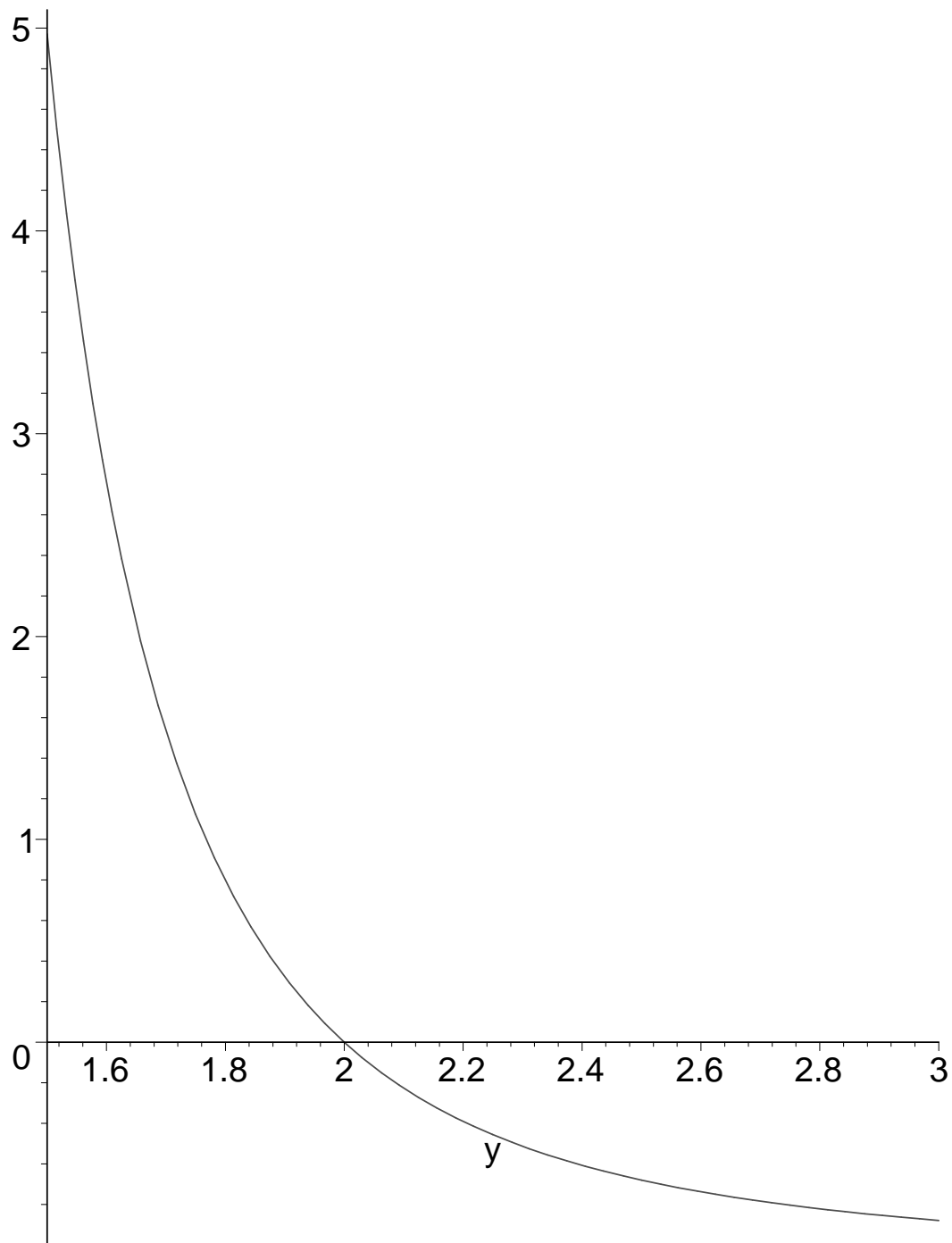
If you don't want to title your appendix, and just call it **Appendix A.** for example, use `\appendix\section*{}` and don't include anything in the title field. This works opposite to the way `\section*` usually works, by including the section number, but not using a title.

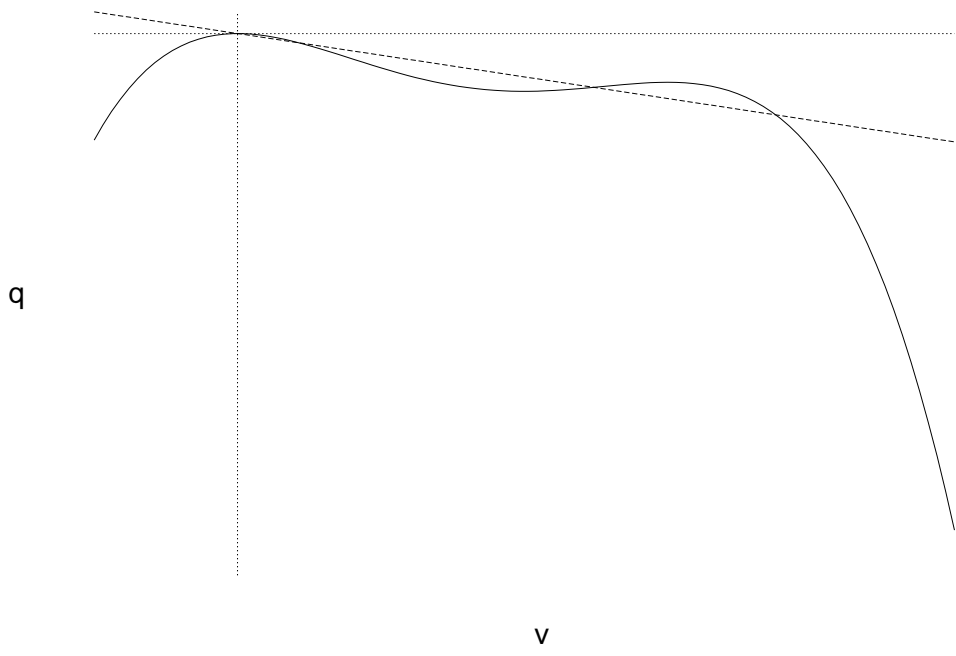
Appendices should appear before the bibliography section, not after, and any acknowledgments should be placed after the appendices and before the bibliography.

REFERENCES

- [1] M. GOOSSENS, F. MITTELBACH, AND A. SAMARIN, *The L^AT_EX Companion*, Addison-Wesley, Reading, MA, 1994.
- [2] N. J. HIGHAM, *Handbook of Writing for the Mathematical Sciences*, Society for Industrial and Applied Mathematics, Philadelphia, PA, 1993.
- [3] L. LAMPORT, *L^AT_EX: A Document Preparation System*, Addison-Wesley, Reading, MA, 1986.
- [4] R. SEROUL AND S. LEVY, *A Beginner's Book of T_EX*, Springer-Verlag, Berlin, New York, 1991.







SAMPLE FILE FOR SIAM L^AT_EX MACRO PACKAGE*

PAUL DUGGAN[†] AND VARIOUS A. U. THORS[‡]

Abstract. An example of SIAM L^AT_EX macros is presented. Various aspects of composing manuscripts for SIAM’s journal series are illustrated with actual examples from accepted manuscripts. SIAM’s stylistic standards are adhered to throughout, and illustrated.

Key words. sign-nonsingular matrix, LU-factorization, indicator polynomial

AMS subject classifications. 15A15, 15A09, 15A23

1. Introduction and examples. This paper presents a sample file for the use of SIAM’s L^AT_EX macro package. It illustrates the features of the macro package, using actual examples culled from various papers published in SIAM’s journals. It is to be expected that this sample will provide examples of how to use the macros to generate standard elements of journal papers, e.g., theorems, definitions, or figures. This paper also serves as an example of SIAM’s stylistic preferences for the formatting of such elements as bibliographic references, displayed equations, and equation arrays, among others. Some special circumstances are not dealt with in this sample file; for such information one should see the included documentation file.

Note: This paper is not to be read in any form for content. The conglomeration of equations, lemmas, and other text elements were put together solely for typographic illustrative purposes and don’t make any sense as lemmas, equations, etc.

1.1. Sample text. Let $S = [s_{ij}]$ ($1 \leq i, j \leq n$) be a $(0, 1, -1)$ -matrix of order n . Then S is a *sign-nonsingular matrix* (SNS-matrix) provided that each real matrix with the same sign pattern as S is nonsingular. There has been considerable recent interest in constructing and characterizing SNS-matrices [1], [4]. There has also been interest in strong forms of sign-nonsingularity [2]. In this paper we give a new generalization of SNS-matrices and investigate some of their basic properties.

Let $S = [s_{ij}]$ be a $(0, 1, -1)$ -matrix of order n and let $C = [c_{ij}]$ be a real matrix of order n . The pair (S, C) is called a *matrix pair of order n* . Throughout, $X = [x_{ij}]$ denotes a matrix of order n whose entries are algebraically independent indeterminates over the real field. Let $S \circ X$ denote the Hadamard product (entrywise product) of S and X . We say that the pair (S, C) is a *sign-nonsingular matrix pair of order n* , abbreviated *SNS-matrix pair of order n* , provided that the matrix

$$A = S \circ X + C$$

is nonsingular for all positive real values of the x_{ij} . If $C = O$ then the pair (S, O) is a SNS-matrix pair if and only if S is a SNS-matrix. If $S = O$ then the pair (O, C) is a SNS-matrix pair if and only if C is nonsingular. Thus SNS-matrix pairs include both nonsingular matrices and sign-nonsingular matrices as special cases.

The pairs (S, C) with

$$S = \begin{bmatrix} 1 & 0 \\ 0 & 0 \end{bmatrix}, \quad C = \begin{bmatrix} 1 & 1 \\ 1 & 1 \end{bmatrix}$$

*This work was supported by the Society for Industrial and Applied Mathematics, Philadelphia, Pennsylvania.

[†]Composition Department, Society for Industrial and Applied Mathematics, 3600 Univeristy City Science Center, Philadelphia, Pennsylvania, 19104-2688 (duggan@siam.org).

[‡]Various Affiliations, supported by various foundation grants.

and

$$S = \begin{bmatrix} 1 & 1 & 0 \\ 1 & 1 & 0 \\ 0 & 0 & 0 \end{bmatrix}, \quad C = \begin{bmatrix} 0 & 0 & 1 \\ 0 & 2 & 0 \\ 3 & 0 & 0 \end{bmatrix}$$

are examples of SNS-matrix pairs.

1.2. A remuneration list. In this paper we consider the evaluation of integrals of the following forms:

$$(1.1) \quad \int_a^b \left(\sum_i E_i B_{i,k,x}(t) \right) \left(\sum_j F_j B_{j,l,y}(t) \right) dt,$$

$$(1.2) \quad \int_a^b f(t) \left(\sum_i E_i B_{i,k,x}(t) \right) dt,$$

where $B_{i,k,x}$ is the i th B-spline of order k defined over the knots $x_i, x_{i+1}, \dots, x_{i+k}$. We will consider B-splines normalized so that their integral is one. The splines may be of different orders and defined on different knot sequences x and y . Often the limits of integration will be the entire real line, $-\infty$ to $+\infty$. Note that (1.1) is a special case of (1.2) where $f(t)$ is a spline.

There are five different methods for calculating (1.1) that will be considered:

1. Use Gauss quadrature on each interval.
2. Convert the integral to a linear combination of integrals of products of B-splines and provide a recurrence for integrating the product of a pair of B-splines.
3. Convert the sums of B-splines to piecewise Bézier format and integrate segment by segment using the properties of the Bernstein polynomials.
4. Express the product of a pair of B-splines as a linear combination of B-splines. Use this to reformulate the integrand as a linear combination of B-splines, and integrate term by term.
5. Integrate by parts.

Of these five, only methods 1 and 5 are suitable for calculating (1.2). The first four methods will be touched on and the last will be discussed at length.

1.3. Some displayed equations and $\{\text{eqnarray}\}$ s. By introducing the product topology on $R^{m \times m} \times R^{n \times n}$ with the induced inner product

$$(1.3) \quad \langle (A_1, B_1), (A_2, B_2) \rangle := \langle A_1, A_2 \rangle + \langle B_1, B_2 \rangle,$$

we calculate the Fréchet derivative of F as follows:

$$(1.4) \quad \begin{aligned} F'(U, V)(H, K) &= \langle R(U, V), H\Sigma V^T + U\Sigma K^T - P(H\Sigma V^T + U\Sigma K^T) \rangle \\ &= \langle R(U, V), H\Sigma V^T + U\Sigma K^T \rangle \\ &= \langle R(U, V)V\Sigma^T, H \rangle + \langle \Sigma^T U^T R(U, V), K^T \rangle. \end{aligned}$$

In the middle line of (1.4) we have used the fact that the range of R is always perpendicular to the range of P . The gradient ∇F of F , therefore, may be interpreted as the pair of matrices:

$$(1.5) \quad \nabla F(U, V) = (R(U, V)V\Sigma^T, R(U, V)^T U\Sigma) \in R^{m \times m} \times R^{n \times n}.$$

Because of the product topology, we know

$$(1.6) \quad \mathcal{T}_{(U,V)}(\mathcal{O}(m) \times \mathcal{O}(n)) = \mathcal{T}_U \mathcal{O}(m) \times \mathcal{T}_V \mathcal{O}(n),$$

where $\mathcal{T}_{(U,V)}(\mathcal{O}(m) \times \mathcal{O}(n))$ stands for the tangent space to the manifold $\mathcal{O}(m) \times \mathcal{O}(n)$ at $(U, V) \in \mathcal{O}(m) \times \mathcal{O}(n)$ and so on. The projection of $\nabla F(U, V)$ onto $\mathcal{T}_{(U,V)}(\mathcal{O}(m) \times \mathcal{O}(n))$, therefore, is the product of the projection of the first component of $\nabla F(U, V)$ onto $\mathcal{T}_U \mathcal{O}(m)$ and the projection of the second component of $\nabla F(U, V)$ onto $\mathcal{T}_V \mathcal{O}(n)$. In particular, we claim that the projection $g(U, V)$ of the gradient $\nabla F(U, V)$ onto $\mathcal{T}_{(U,V)}(\mathcal{O}(m) \times \mathcal{O}(n))$ is given by the pair of matrices:

$$(1.7) \quad g(U, V) = \left(\frac{R(U, V)V\Sigma^T U^T - U\Sigma V^T R(U, V)^T}{2} U, \right. \\ \left. \frac{R(U, V)^T U\Sigma V^T - V\Sigma^T U^T R(U, V)}{2} V \right).$$

Thus, the vector field

$$(1.8) \quad \frac{d(U, V)}{dt} = -g(U, V)$$

defines a steepest descent flow on the manifold $\mathcal{O}(m) \times \mathcal{O}(n)$ for the objective function $F(U, V)$.

2. Main results. Let (S, C) be a matrix pair of order n . The determinant

$$\det(S \circ X + C)$$

is a polynomial in the indeterminates of X of degree at most n over the real field. We call this polynomial the *indicator polynomial* of the matrix pair (S, C) because of the following proposition.

THEOREM 2.1. *The matrix pair (S, C) is a SNS-matrix pair if and only if all the nonzero coefficients in its indicator polynomial have the same sign and there is at least one nonzero coefficient.*

Proof. Assume that (S, C) is a SNS-matrix pair. Clearly the indicator polynomial has a nonzero coefficient. Consider a monomial

$$(2.1) \quad b_{i_1, \dots, i_k; j_1, \dots, j_k} x_{i_1 j_1} \cdots x_{i_k j_k}$$

occurring in the indicator polynomial with a nonzero coefficient. By taking the x_{ij} that occur in (2.1) large and all others small, we see that any monomial that occurs in the indicator polynomial with a nonzero coefficient can be made to dominate all others. Hence all the nonzero coefficients have the same sign. The converse is immediate. \square

For SNS-matrix pairs (S, C) with $C = O$ the indicator polynomial is a homogeneous polynomial of degree n . In this case Theorem 2.1 is a standard fact about SNS-matrices.

LEMMA 2.2 (Stability). *Given $T > 0$, suppose that $\|\epsilon(t)\|_{1,2} \leq h^{q-2}$ for $0 \leq t \leq T$ and $q \geq 6$. Then there exists a positive number B that depends on T and the exact solution ψ only such that for all $0 \leq t \leq T$,*

$$(2.2) \quad \frac{d}{dt} \|\epsilon(t)\|_{1,2} \leq B(h^{q-3/2} + \|\epsilon(t)\|_{1,2}).$$

The function $B(T)$ can be chosen to be nondecreasing in time.

THEOREM 2.3. *The maximum number of nonzero entries in a SNS-matrix S of order n equals*

$$\frac{n^2 + 3n - 2}{2}$$

with equality if and only if there exist permutation matrices such that $P|S|Q = T_n$ where

$$(2.3) \quad T_n = \begin{bmatrix} 1 & 1 & \cdots & 1 & 1 & 1 \\ 1 & 1 & \cdots & 1 & 1 & 1 \\ 0 & 1 & \cdots & 1 & 1 & 1 \\ \vdots & \vdots & \ddots & \vdots & \vdots & \vdots \\ 0 & 0 & \cdots & 1 & 1 & 1 \\ 0 & 0 & \cdots & 0 & 1 & 1 \end{bmatrix}.$$

We note for later use that each submatrix of T_n of order $n - 1$ has all 1s on its main diagonal.

We now obtain a bound on the number of nonzero entries of S in a SNS-matrix pair (S, C) in terms of the degree of the indicator polynomial. We denote the strictly upper triangular $(0,1)$ -matrix of order m with all 1s above the main diagonal by U_m . The all 1s matrix of size m by p is denoted by $J_{m,p}$.

PROPOSITION 2.4 (Convolution theorem). *Let*

$$a * u(t) = \int_0^t a(t - \tau)u(\tau)d\tau, \quad t \in (0, \infty).$$

Then

$$\widehat{a * u}(s) = \widehat{a}(s)\widehat{u}(s).$$

LEMMA 2.5. *For $s_0 > 0$, if*

$$\int_0^\infty e^{-2s_0 t} v^{(1)}(t)v(t)dt \leq 0,$$

then

$$\int_0^\infty e^{-2s_0 t} v^2(t)dt \leq \frac{1}{2s_0} v^2(0).$$

Proof. Applying integration by parts, we obtain

$$\begin{aligned} \int_0^\infty e^{-2s_0 t} [v^2(t) - v^2(0)]dt &= \lim_{t \rightarrow \infty} \left(-\frac{1}{2s_0} e^{-2s_0 t} v^2(t) \right) + \frac{1}{s_0} \int_0^\infty e^{-2s_0 t} v^{(1)}(t)v(t)dt \\ &\leq \frac{1}{s_0} \int_0^\infty e^{-2s_0 t} v^{(1)}(t)v(t)dt \leq 0. \end{aligned}$$

Thus

$$\int_0^\infty e^{-2s_0 t} v^2(t)dt \leq v^2(0) \int_0^\infty e^{-2s_0 t} dt = \frac{1}{2s_0} v^2(0). \quad \square$$

COROLLARY 2.6. Let \mathbf{E} satisfy (5)–(6) and suppose \mathbf{E}^h satisfies (7) and (8) with a general \mathbf{G} . Let $\mathbf{G} = \nabla \times \Phi + \nabla p$, $p \in H_0^1(\Omega)$. Suppose that ∇p and $\nabla \times \Phi$ satisfy all the assumptions of Theorems 4.1 and 4.2, respectively. In addition suppose all the regularity assumptions of Theorems 4.1–4.2 are satisfied. Then for $0 \leq t \leq T$ and $0 < \epsilon \leq \epsilon_0$ there exists a constant $C = C(\epsilon, T)$ such that

$$\|(\mathbf{E} - \mathbf{E}^h)(t)\|_0 \leq Ch^{k+1-\epsilon},$$

where C also depends on the constants given in Theorems 4.1 and 4.2.

DEFINITION 2.7. Let S be an isolated invariant set with isolating neighborhood N . An index pair for S is a pair of compact sets (N_1, N_0) with $N_0 \subset N_1 \subset N$ such that:

- (i) $cl(N_1 \setminus N_0)$ is an isolating neighborhood for S .
- (ii) N_i is positively invariant relative to N for $i = 0, 1$, i.e., given $x \in N_i$ and $x \cdot [0, t] \subset N$, then $x \cdot [0, t] \subset N_i$.
- (iii) N_0 is an exit set for N_1 , i.e. if $x \in N_1$, $x \cdot [0, \infty) \not\subset N_1$, then there is a $T \geq 0$ such that $x \cdot [0, T] \subset N_1$ and $x \cdot T \in N_0$.

2.1. Numerical experiments. We conducted numerical experiments in computing inexact Newton steps for discretizations of a *modified Bratu problem*, given by

$$(2.4) \quad \begin{aligned} \Delta w + ce^w + d \frac{\partial w}{\partial x} &= f \quad \text{in } D, \\ w &= 0 \quad \text{on } \partial D, \end{aligned}$$

where c and d are constants. The actual Bratu problem has $d = 0$ and $f \equiv 0$. It provides a simplified model of nonlinear diffusion phenomena, e.g., in combustion and semiconductors, and has been considered by Glowinski, Keller, and Rheinhardt [11], as well as by a number of other investigators; see [11] and the references therein. See also problem 3 by Glowinski and Keller and problem 7 by Mittelmann in the collection of nonlinear model problems assembled by Moré [13]. The modified problem (2.4) has been used as a test problem for inexact Newton methods by Brown and Saad [7].

In our experiments, we took $D = [0, 1] \times [0, 1]$, $f \equiv 0$, $c = d = 10$, and discretized (2.4) using the usual second-order centered differences over a 100×100 mesh of equally spaced points in D . In GMRES(m), we took $m = 10$ and used fast Poisson right preconditioning as in the experiments in §2. The computing environment was as described in §2. All computing was done in double precision.

In the first set of experiments, we allowed each method to run for 40 GMRES(m) iterations, starting with zero as the initial approximate solution, after which the limit of residual norm reduction had been reached. The results are shown in Fig. 2.1. In Fig. 2.1, the top curve was produced by method FD1. The second curve from the top is actually a superposition of the curves produced by methods EHA2 and FD2; the two curves are visually indistinguishable. Similarly, the third curve from the top is a superposition of the curves produced by methods EHA4 and FD4, and the fourth curve from the top, which lies barely above the bottom curve, is a superposition of the curves produced by methods EHA6 and FD6. The bottom curve was produced by method A.

In the second set of experiments, our purpose was to assess the relative amount of computational work required by the methods which use higher-order differencing to reach comparable levels of residual norm reduction. We compared pairs of methods

FIG. 2.1. \log_{10} of the residual norm versus the number of GMRES(m) iterations for the finite difference methods.

TABLE 2.1

Statistics over 20 trials of GMRES(m) iteration numbers, F -evaluations, and run times required to reduce the residual norm by a factor of ϵ . For each method, the number of GMRES(m) iterations and F -evaluations was the same in every trial.

Method	ϵ	Number of Iterations	Number of F -Evaluations	Mean Run Time (Seconds)	Standard Deviation
EHA2	10^{-10}	26	32	47.12	.1048
FD2	10^{-10}	26	58	53.79	.1829
EHA4	10^{-12}	30	42	56.76	.1855
FD4	10^{-12}	30	132	81.35	.3730
EHA6	10^{-12}	30	48	58.56	.1952
FD6	10^{-12}	30	198	100.6	.3278

EHA2 and FD2, EHA4 and FD4, and EHA6 and FD6 by observing in each of 20 trials the number of GMRES(m) iterations, number of F -evaluations, and run time required by each method to reduce the residual norm by a factor of ϵ , where for each pair of methods ϵ was chosen to be somewhat greater than the limiting ratio of final to initial residual norms obtainable by the methods. In these trials, the initial approximate solutions were obtained by generating random components as in the similar experiments in §2. We note that for every method, the numbers of GMRES(m) iterations and F -evaluations required before termination did not vary at all over the 20 trials. The GMRES(m) iteration counts, numbers of F -evaluations, and means and standard deviations of the run times are given in Table 2.1.

In our first set of experiments, we took $c = d = 10$ and used right preconditioning with a fast Poisson solver from FISHPACK [16], which is very effective for these fairly small values of c and d . We first started each method with zero as the initial approximate solution and allowed it to run for 40 GMRES(m) iterations, after which the limit of residual norm reduction had been reached. Figure 2.2 shows plots of the logarithm of the Euclidean norm of the residual versus the number of GMRES(m) iterations for the three methods. We note that in Fig. 2.2 and in all other figures below, the plotted residual norms were not the values maintained by GMRES(m), but rather were computed as accurately as possible “from scratch.” That is, at each

FIG. 2.2. \log_{10} of the residual norm versus the number of GMRES(m) iterations for $c = d = 10$ with fast Poisson preconditioning. Solid curve: Algorithm EHA; dotted curve: FDP method; dashed curve: FSP method.

GMRES(m) iteration, the current approximate solution was formed and its product with the coefficient matrix was subtracted from the right-hand side, all in double precision. It was important to compute the residual norms in this way because the values maintained by GMRES(m) become increasingly untrustworthy as the limits of residual norm reduction are neared; see [17]. It is seen in Fig. 2.2 that Algorithm EHA achieved the same ultimate level of residual norm reduction as the FDP method and required only a few more GMRES(m) iterations to do so.

In our second set of experiments, we took $c = d = 100$ and carried out trials analogous to those in the first set above. No preconditioning was used in these experiments, both because we wanted to compare the methods without preconditioning and because the fast Poisson preconditioning used in the first set of experiments is not cost effective for these large values of c and d . We first allowed each method to run for 600 GMRES(m) iterations, starting with zero as the initial approximate solution, after which the limit of residual norm reduction had been reached.

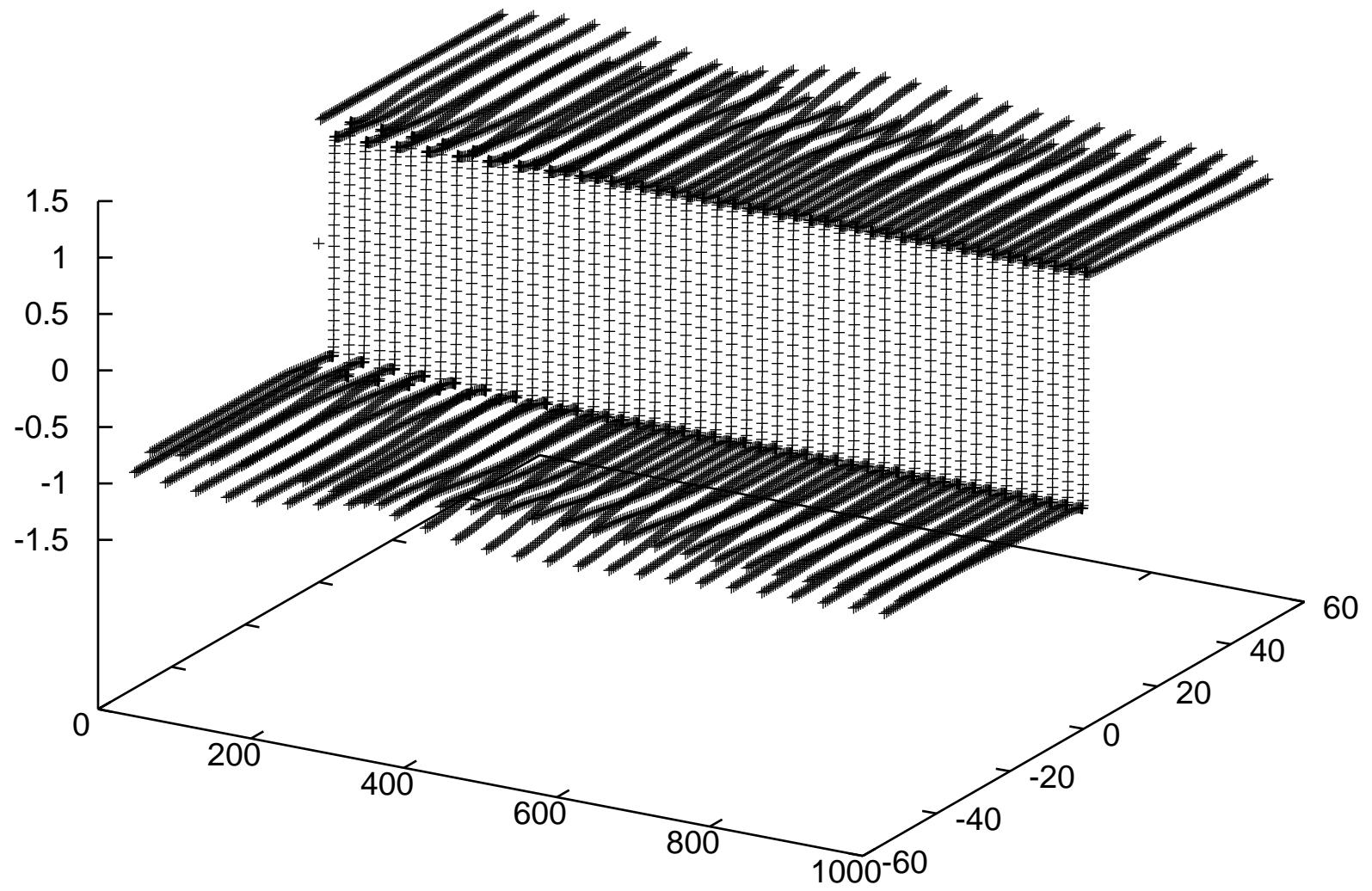
Acknowledgments. The author thanks the anonymous authors whose work largely constitutes this sample file. He also thanks the INFO-TeX mailing list for the valuable indirect assistance he received.

REFERENCES

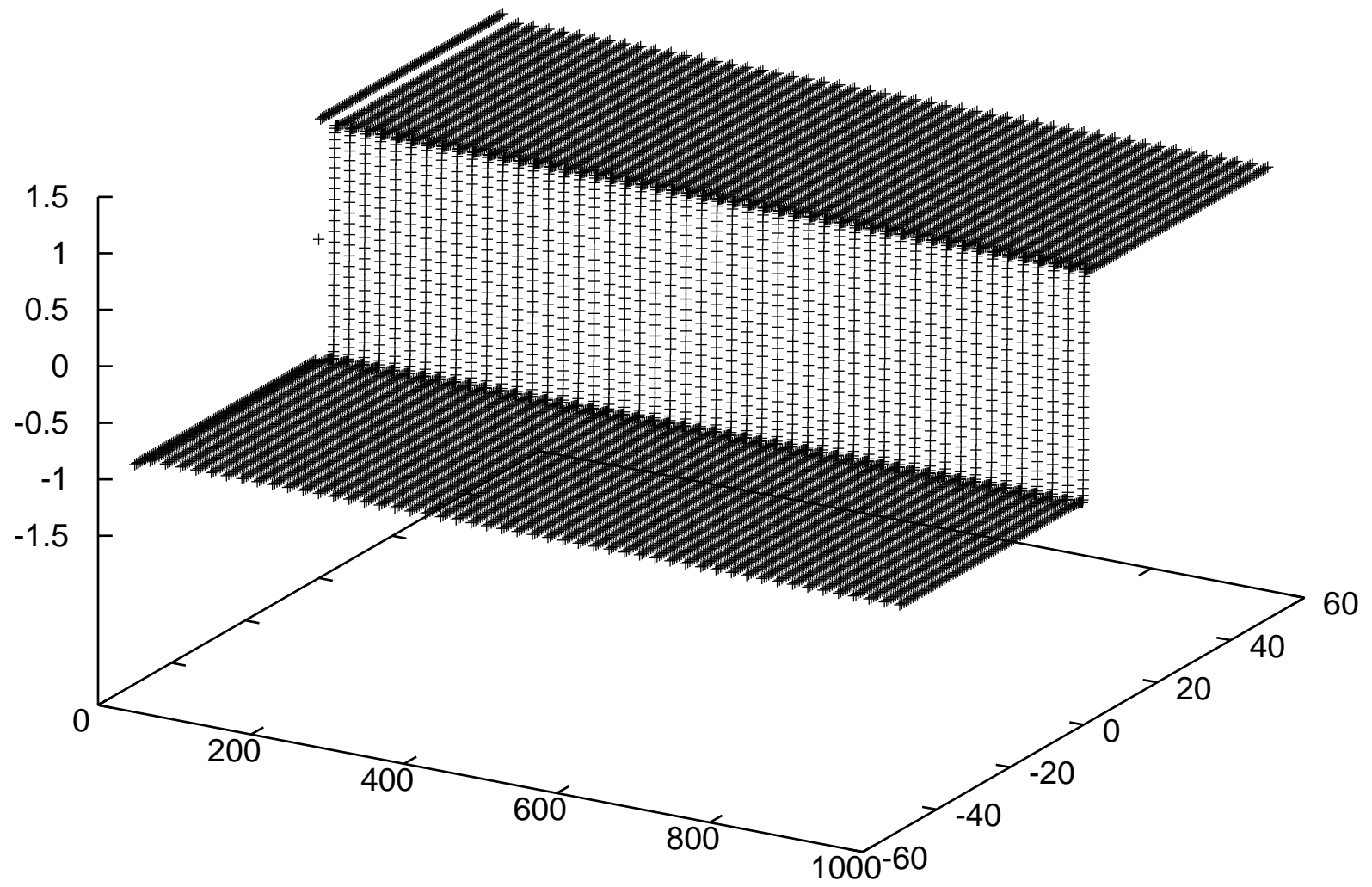
- [1] R. A. BRUALDI AND B. L. SHADER, *On sign-nonsingular matrices and the conversion of the permanent into the determinant*, in Applied Geometry and Discrete Mathematics, The Victor Klee Festschrift, P. Gritzmann and B. Sturmfels, eds., American Mathematical Society, Providence, RI, 1991, pp. 117–134.
- [2] J. DREW, C. R. JOHNSON, AND P. VAN DEN DRIESSCHE, *Strong forms of nonsingularity*, Linear Algebra Appl., 162 (1992), to appear.
- [3] P. M. GIBSON, *Conversion of the permanent into the determinant*, Proc. Amer. Math. Soc., 27 (1971), pp. 471–476.

- [4] V. KLEE, R. LADNER, AND R. MANBER, *Signsolvability revisited*, Linear Algebra Appl., 59 (1984), pp. 131–157.
- [5] K. MUROTA, *LU-decomposition of a matrix with entries of different kinds*, Linear Algebra Appl., 49 (1983), pp. 275–283.
- [6] O. AXELSSON, *Conjugate gradient type methods for unsymmetric and inconsistent systems of linear equations*, Linear Algebra Appl., 29 (1980), pp. 1–16.
- [7] P. N. BROWN AND Y. SAAD, *Hybrid Krylov methods for nonlinear systems of equations*, SIAM J. Sci. Statist. Comput., 11 (1990), pp. 450–481.
- [8] R. S. DEMBO, S. C. EISENSTAT, AND T. STEIHAUG, *Inexact Newton methods*, SIAM J. Numer. Anal., 19 (1982), pp. 400–408.
- [9] S. C. EISENSTAT, H. C. ELMAN, AND M. H. SCHULTZ, *Variational iterative methods for nonsymmetric systems of linear equations*, SIAM J. Numer. Anal., 20 (1983), pp. 345–357.
- [10] H. C. ELMAN, *Iterative methods for large, sparse, nonsymmetric systems of linear equations*, Ph.D. thesis, Department of Computer Science, Yale University, New Haven, CT, 1982.
- [11] R. GLOWINSKI, H. B. KELLER, AND L. RHEINHART, *Continuation-conjugate gradient methods for the least-squares solution of nonlinear boundary value problems*, SIAM J. Sci. Statist. Comput., 6 (1985), pp. 793–832.
- [12] G. H. GOLUB AND C. F. VAN LOAN, *Matrix Computations*, Second ed., The Johns Hopkins University Press, Baltimore, MD, 1989.
- [13] J. J. MORÉ, *A collection of nonlinear model problems*, in Computational Solutions of Nonlinear Systems of Equations, E. L. Allgower and K. Georg, eds., Lectures in Applied Mathematics, Vol. 26, American Mathematical Society, Providence, RI, 1990, pp. 723–762.
- [14] Y. SAAD, *Krylov subspace methods for solving large unsymmetric linear systems*, Math. Comp., 37 (1981), pp. 105–126.
- [15] Y. SAAD AND M. H. SCHULTZ, *GMRES: A generalized minimal residual method for solving nonsymmetric linear systems*, SIAM J. Sci. Statist. Comput., 7 (1986), pp. 856–869.
- [16] P. N. SWARZTRAUBER AND R. A. SWEET, *Efficient FORTRAN subprograms for the solution of elliptic partial differential equations*, ACM Trans. Math. Software, 5 (1979), pp. 352–364.
- [17] H. F. WALKER, *Implementation of the GMRES method using Householder transformations*, SIAM J. Sci. Statist. Comput., 9 (1988), pp. 152–163.
- [18] ———, *Implementations of the GMRES method*, Computer Phys. Comm., 53 (1989), pp. 311–320.

"RESULT1" +



"RESULT2" +



"RESULT5" +

